UNIVERSIDAD DE CONCEPCIÓN

Centro de Investigación en Ingeniería Matemática (CI²MA)

Mathematical analysis and numerical solution of axisymmetric eddy-current problems with Preisach hysteresis model

Alfredo Bermúdez, Dolores Gómez,
Rodolfo Rodríguez, Pablo Venegas

SERIE DE PRE-PUBLICACIONES

MATHEMATICAL ANALYSIS AND NUMERICAL SOLUTION OF AXISYMMETRIC EDDY-CURRENT PROBLEMS WITH PREISACH HYSTERESIS MODEL*

Alfredo Bermúdez, Dolores Gómez †

Departamento de Matemática Aplicada
Universidade de Santiago de Compostela
Spain

Rodolfo Rodríguez, Pablo Venegas‡

CI²MA, Departamento de Ingeniería Matemática
Universidad de Concepción
Chile

January 2, 2014

1 Introduction

This work deals with the mathematical analysis and the numerical computation of transient electromagnetic fields in nonlinear magnetic media with hysteresis.

The phenomenon of hysteresis has been observed for a long time in many different areas of science and engineering and, in particular, in the area of magnetism. Many ferromagnetic materials present this behavior which essentially means that the magnetic induction at each particular point depends not only on its present magnetic intensity, but also on the past magnetic history of the volume element under consideration. Thus, building a mathematical model of the magnetic constitutive law is a very difficult task and numerical simulation of devices involving ferromagnetic materials is still quite a challenge.

From the physical point of view one must distinguish between scalar hysteresis models and vectorial hysteresis models. Scalar models correspond to the cases where magnetic induction and magnetic field are aligned at any position and at any time. On the contrary, if the magnetic field and the magnetic induction may be non-collinear, a vectorial model must be considered. In this work we will restrict ourselves to scalar hysteresis models.

The results presented in this work complement those in [3, 4], where the mathematical and numerical analysis of a two-dimensional (2D) nonlinear axisymmetric eddy current model was performed under fairly general assumptions on the H-B curve, but without considering hysteresis effects. Now, the constitutive relation between H and B is given by a

†Electronic address: `alfredo.bermudez@usc.es, mdolores.gomez@usc.es`
‡Electronic address: `rodolfo@ing-mat.udec.cl, pvenegas@ing-mat.udec.cl`

rather general hysteresis operator. Like in [3, 4], we assume axisymmetry of the fields and in view of applications we also consider that the source inputs are current intensities or voltage drops. With this in mind, two source terms are considered: either the magnetic field on the boundary (Dirichlet condition) or the magnetic flux across a meridian section of the device (magnetic flux condition) are given. These source terms are physically realistic in the sense that there are many real applications where they can be readily obtained from measurable quantities (see [9, 1, 2, 22, 19, 28]). Moreover, we consider a time and space dependent electrical conductivity, an important issue because this quantity is typically a function of temperature which, in its turn, is a time dependent field. For both problems, an existence result is achieved under suitable assumptions.

For the numerical solution, we consider the classical Preisach model as hysteresis operator, a finite element discretization by piecewise linear functions on triangular meshes, and the backward Euler scheme for time discretization.

In the context of parabolic equations with hysteresis there are several publications devoted to the mathematical analysis of the problem (see, [32, 33, 34, 16, 27] and more recently [10, 13, 11]). In particular, [13] deals with an abstract parabolic equation motivated by a 2D eddy current model with hysteresis, but the numerical analysis and computer implementation of the problem are not considered. Numerical approximation of parabolic problems with hysteresis are considered, for instance, in [30, 31]. In the context of the computational methods for 2D eddy current models with hysteresis we mention [28, 29]. However, to the best of the authors' knowledge, the parabolic problem presented in [28] has not been mathematically analyzed yet.

In the present work, by using appropriate weighted two-dimensional Sobolev spaces for axisymmetric problems, we prove the existence of solution to a weak formulation in terms of the magnetic field. The method used for this purpose is the Rothe's method that consists of introducing an implicit time discretization, obtaining a priori estimates and then passing to the limit as the time-step goes to zero (see [25]). This approximation procedure is often used in the analysis of equations including a memory operator (see, for instance, [11, 34]) because at each time step we deal with a stationary problem where the memory operator is reduced to a nonlinear operator of the unknown field at this time step. In particular, we base our proof on arguments given in [34] where existence of solution to a homogeneous Dirichlet problem is achieved. Let us remark that, to the best of the author's knowledge, the problems addressed in this paper do not fit in this or other existing results because, on the one hand, in our case the coefficients depend on time and, on the other hand, different boundary conditions are considered.

The outline of this work is as follows: in Section 2 and Section 3 we recall, respectively, some basic principles of magnetic hysteresis and the properties of hysteresis operators that will be used in the mathematical analysis of the problem. To make the document self-contained, in Section 4 we include a detailed description of the classical Preisach model following Mayergoyz [20]. In particular, we recall the method to identify, for a particular magnetic material, the function defining the associated Preisach operator.

Next, in Section 5, we introduce the transient eddy current model with hysteresis to be analyzed. The axisymmetric case is considered and the two alternative types of source terms are introduced. In Section 6, after recalling some analytical tools, weak formulations are obtained. Then, existence of solution is proved for both formulations. Section 7 is devoted to the numerical implementation of the fully-discrete problem arising from backward Euler time-discretization and a finite element method for space discretization. Finally, in Section 8, a numerical test is reported.

2

2 Magnetic hysteresis

Ferromagnetic materials are very sensitive to be magnetized. These materials are made up of small regions known as *magnetic domains*. Domains are very small regions in the material structure, where all the dipoles are paralleled in the same direction. In each domain, all of the atomic dipoles are coupled together in a preferential direction (see Figure 1 (left)). In other words, the domains are like small permanent magnets oriented randomly in the material.

Ferromagnetic materials become magnetized when the magnetic domains within the material are aligned (see Figure 1 (right)). This can be done by subjecting the material to a strong external magnetic field or by passing electrical current through it. Then, some or all of the domains can become aligned. The more the aligned domains, the stronger the magnetic field in the material. When all of the domains are aligned, the material is said to be magnetically saturated. This means that no additional amount of external magnetization force will cause an increase in its internal level of magnetization. After removing this external field, most of the domains come back to random positions, but a few of them still remain in their changed position. Because of these unchanged domains the substance becomes slightly magnetized permanently. The phenomenon which causes B to lag behind H, so that the magnetization curve for increasing and decreasing fields is not the same, is called hysteresis and the loop traced out by the magnetization curve is called a *hysteresis cycle* or *hysteresis loop*.
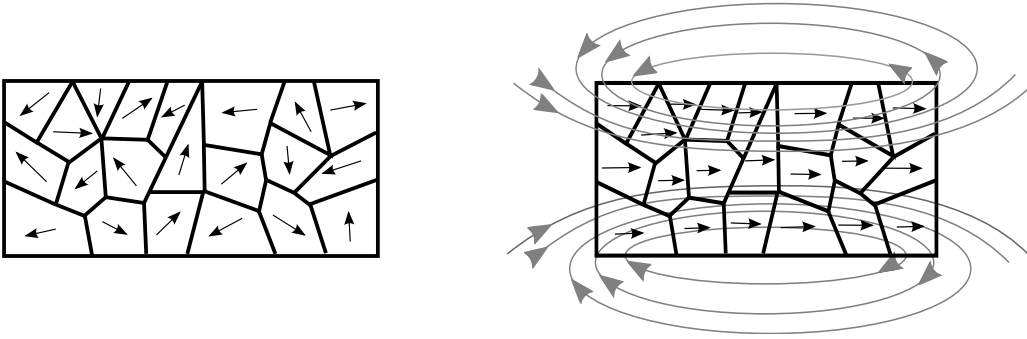

Figure 1: Randomly oriented domains (left) and aligned domains (right).

Figure 2 shows an example of a hysteresis loop. In this loop we represent the relationship between the induced magnetic flux density B and the magnetizing field H. It is often referred to as the B-H loop.

The loop is generated by measuring the magnetic flux of a ferromagnetic material while the magnetizing field is changing. We start at the *demagnetized* state, that is, when a ferromagnetic material has never been previously magnetized or has been thoroughly demagnetized.

We consider a demagnetized ferromagnetic material subjected to a monotonically increasing magnetic field starting from zero. Then, the couples $(H(t), B(t))$ describe the curve labelled 1 shown in Figure 2. Thus, the magnetic induction also increases up to a maximum value B_m at which *saturation* is attained. This curve is called *initial* (or *normal*) magnetization curve.

Next, we decrease *monotonically* the magnetic field from the saturation value H_m to the opposite saturation value $-H_m$. Then, points $(H(t), B(t))$ do not trace back the above initial curve but follow curve labelled 2 until the magnetic field attains the value $-H_m$. If we increase again the magnetic field, then points $(H(t), B(t))$ describe curve labelled 3. More
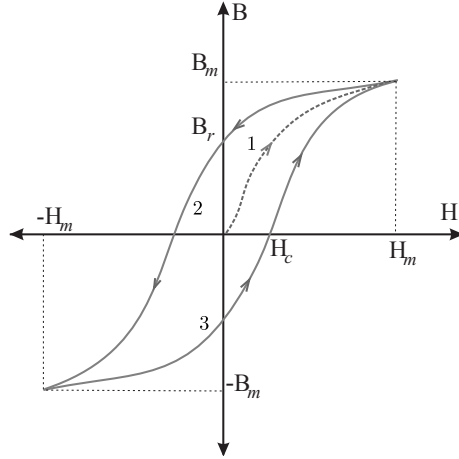
Figure 2: Magnetic hysteresis.

generally, if the magnetic field oscillates between two extreme and opposite values H_m and $-H_m$ monotonically (i.e., $H(t)$ does not have any local extrema apart from the global ones) then the couples $(H(t), B(t))$ follow alternatively curves 2 and 3 in the indicated sense, i.e., they travel along the so-called hysteresis *major loop*.

Two important quantities are related with ferromagnetic materials: the *remanence* and the *coercive fields*. Remanence represents the magnetization after applying a large magnetic field and then removing it. Thus, it corresponds to the remanent magnetic induction denoted by B_r in Figure 2. In its turn, the coercive field is the intensity of the magnetic field needed to bring the magnetization from the remanent value to zero, i.e., the value H_c in Figure 2.
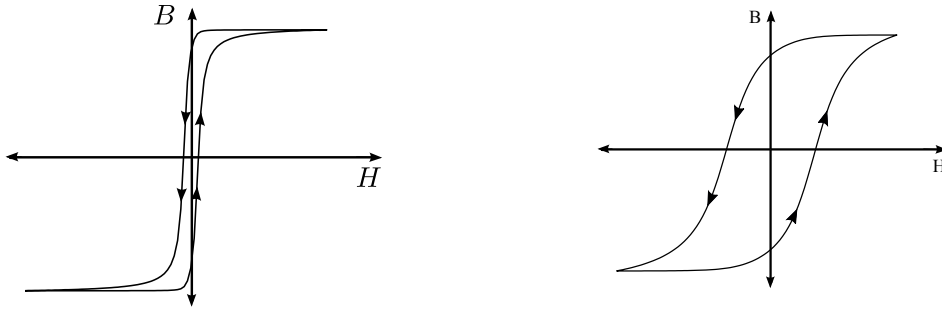

Figure 3: Hysteresis loops for soft (left) and hard (right) magnetic materials.

According to these parameters, ferromagnetic materials can be classified in *soft* and *hard* magnetic materials. Soft magnetic materials have small coercive fields, so they are easy to magnetize and their hysteresis loops are thin. On the contrary, hard magnetic materials have large coercive fields and they tend to stay magnetized, while soft materials do not (see Figure 3).

3 Hysteresis operators

3.1 Basic properties

The hysteresis phenomenon is present not only in electromagnetism but also in different areas of science such as mechanics, among others. Hysteresis modelling early work date back to 1935 and was proposed by the physicist F. Preisach [23] in the context of ferromagnetism.

From the mathematical point of view, we refer to the monograph of mathematicians Krasnosel'skiĭ and Pokrovskiĭ [18] as well as to the books by Visintin [34] and Brokate [8] and, from a physical point of view, to Mayergoyz [20] and Bertotti [6].

In this section, we recall some basic background material on hysteresis operators based on the description given in [34], which will be used in the sequel.

Let us start by considering a simple setting, namely, a system whose state is characterized by two scalar variables, u and w, both of them depending on time t. Let us suppose that the evolution of w is determined by the one of u.

For instance, in Figure 4, if u increases from u_1 to u_2, the pair (u, w) moves along the monotone curve abc. Conversely, if u decreases from u_2 to u_1, then (u, w) moves along a different monotone curve cda. Moreover, if u inverts its motion when $u_1 < u(t) < u_2$, then (u, w) moves inside of the hysteresis region, namely, the part of the (u, w)-plane that is bounded by the major loop $abcd$. Here we assume that pair (u, w) moves along continuous curves so we speak of continuous hysteresis. Although most typical examples of hysteresis phenomena exhibit hysteresis loops, the occurrence of loops should not be regarded as an essential feature of hysteresis.
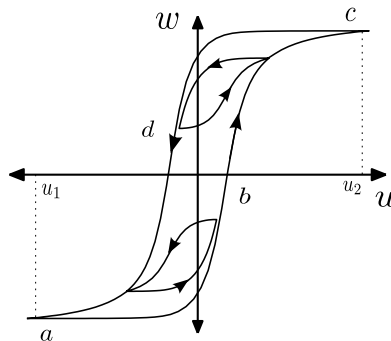

Figure 4: Hysteresis loop.

According to [34], we can distinguish two main characteristics of hysteresis phenomena: the *memory effect* and the *rate independence*.

To illustrate these concepts, we consider the (u, w) relation introduced above. The *memory effect* means that, at any instant t, the value of $w(t)$ depends on the previous evolution of u rather than only on $u(t)$. On the other hand, *rate independence* means that, at any instant t, $w(t)$ depends just on the range of function $u : [0, t] \to \mathbb{R}$ and on the order in which the values of u before t have been attained. In other words, w does not depend on the *velocity* of u.

We notice that, even in most typical hysteresis phenomena, like ferromagnetism, ferroelectricity or plasticity, memory effects are not purely rate independent, since hysteresis is coupled with viscous-type effects. However, in several cases the rate independent component prevails, provided that evolution is not too fast.

In order to introduce a functional setting for hysteresis operators, we first notice that, at any instant t, $w(t)$ will depend not only on the previous evolution of u (i.e., on $u|_{[0,t]}$) but also on the "initial state" of the system. Due to the memory dependence of hysteresis processes, additional information is needed to make up for the lack of history when the process begins. This initial information must represent the "history" of function u before $t = 0$. Hence, not only the standard initial value $(u(0), w(0))$ must be provided. In general, we consider a

5

variable ξ containing all the information about the "initial state". For instance, we express this as follows:

$$\widetilde{\mathcal{F}} : C([0,T]) \times Y \to C([0,T])$$
$$(u,\xi) \to w = \widetilde{\mathcal{F}}(u,\xi)$$

with Y a suitable metric space. Thus, $\widetilde{\mathcal{F}}(\cdot,\xi)$ represents an operator between spaces of time-dependent functions, for each fixed ξ.

We introduce the following definitions related to the previous discussion.

An operator $\widetilde{\mathcal{F}}(\cdot,\xi)$ is said to be *causal* if for any $t \in [0,T]$, the output $w(t) = [\widetilde{\mathcal{F}}(u,\xi)](t)$ is independent of $u|_{[t,T]}$, i.e.,

$$\forall (u_1,\xi), (u_2,\xi) \in \text{Dom}(\widetilde{\mathcal{F}}),$$
$$u_1|_{[0,t]} = u_2|_{[0,t]} \Rightarrow [\widetilde{\mathcal{F}}(u_1,\xi)](t) = [\widetilde{\mathcal{F}}(u_2,\xi)](t) \quad \forall t \in (0,T].$$

We require the path of the pair (u,w) to be invariant with respect to any increasing diffeomorphism $\varphi : [0,T] \to [0,T]$, i.e.,

$$\forall (u,\xi) \in \text{Dom}(\widetilde{\mathcal{F}}),$$
$$\widetilde{\mathcal{F}}(u \circ \varphi, \xi) = \widetilde{\mathcal{F}}(u,\xi) \circ \varphi \quad \text{in } [0,T].$$

This means that at any instant t, $w(t)$ only depends on $u|_{[0,t]}$ and on the order in which the values of u have been attained before t (*rate independence*).

We characterize a *hysteresis operator* as a causal and rate independent operator.

In what follows we shall deal with hysteresis operators that are continuous in the following sense:

$$\forall \left\{ (u_n, \xi_n), \in \text{Dom}(\widetilde{\mathcal{F}}) \right\}_{n \in \mathbb{N}}, \text{ if } u_n \to u \text{ uniformly in } [0,T] \text{ and } \xi_n \to \xi \text{ in } Y,$$
$$\text{then } \widetilde{\mathcal{F}}(u_n, \xi_n) \to \widetilde{\mathcal{F}}(u,\xi) \text{ uniformly in } [0,T]. \tag{3.1}$$

Another property which may be fulfilled by hysteresis operators is *order preservation*, that is,

$$\forall (u_1, \xi_1), (u_2, \xi_2), \in \text{Dom}(\widetilde{\mathcal{F}}), \text{ if } u_1 \le u_2 \text{ and } \xi_1 \le \xi_2,$$
$$\text{then } |[\widetilde{\mathcal{F}}(u_1, \xi_1)](t)| \le |[\widetilde{\mathcal{F}}(u_2, \xi_2)](t)| \quad \forall t \in (0,T]. \tag{3.2}$$

Moreover, it is also natural to require the following property, usually named *piecewise monotonicity*:

$$\forall (u,\xi) \in \text{Dom}(\widetilde{\mathcal{F}}), \forall [t_1, t_2] \subset [0,T],$$
$$\text{if } u \text{ is either nondecreasing or nonincreasing in } [t_1, t_2], \text{ then so is } \widetilde{\mathcal{F}}(u,\xi). \tag{3.3}$$

We notice that the classical L^2-monotonicity property

$$\int_0^T \left([\widetilde{\mathcal{F}}(u_1,\xi)](t) - [\widetilde{\mathcal{F}}(u_2,\xi)](t) \right) (u_1(t) - u_2(t)) \, dt \ge 0 \qquad \forall u_1, u_2 \in \text{Dom}(\widetilde{\mathcal{F}})$$

is a too strong requirement for hysteresis operators. Actually, a rate independent operator is monotone with respect to the usual scalar product of $L^2(0,T)$ only if it is of the form $\widetilde{\mathcal{F}}(u,\xi) = \varphi \circ u$ for some function $\varphi : \mathbb{R} \to \mathbb{R}$ (see [7, Chapter I]).

6

3.2 Space and time dependence

The hysteresis operators introduced in the above section work between spaces of continuous functions, i.e.,

$$\widetilde{\mathcal{F}} : C([0,T]) \times Y \to C([0,T]),$$

where we recall that Y is a suitable metric space containing all the information about the desired "initial state". These operators are usually employed in problems in which time is the only independent variable, like in the case of ordinary differential equations. In the case of partial differential equations, these operators cannot be directly applied and it is necessary to define a suitable operator $\mathcal{F}$ acting between function spaces involving the space variable.

To begin with, we first define appropriate Lebesgue spaces that will be used for the mathematical analysis of the problem (see [34, Section XII.2]).

Let Q be a Banach space and Ω an open subset of $\mathbb{R}^N (N \geq 1)$ with Lipschitz continuous boundary. We define $\mathcal{S}(\Omega; Q)$ to be the family of *simple functions* $\Omega \to Q$, namely, functions with finite range such that the inverse image of any element of Q is measurable. Then, we introduce the space of strongly measurable functions:

$$\mathcal{M}(\Omega; Q) := \Big\{ v : \Omega \to Q : \exists \{v_n \in \mathcal{S}(\Omega; Q)\}_{n \in \mathbb{N}} \text{ such that }$$

$$v_n \to v \text{ strongly in } Q \text{ a.e. in } \Omega \Big\}.$$

Now, we are in a position to introduce a space-time hysteresis operator. Given a hysteresis operator $\widetilde{\mathcal{F}}$, we introduce, for any $u : \Omega \times [0,T] \to \mathbb{R}$ such that $u(x, \cdot) \in C([0,T])$ and any $\xi : \Omega \to Y$, the corresponding space dependent operator $\mathcal{F} : \mathcal{M}(\Omega; C([0,T]) \times Y) \to \mathcal{M}(\Omega; C([0,T]))$ as follows

$$[\mathcal{F}(u,\xi)](x,t) := [\widetilde{\mathcal{F}}(u(x,\cdot), \xi(x))](t), \qquad \forall t \in [0,T], \text{ a.e in } \Omega.$$

We notice that operator $\widetilde{\mathcal{F}}$ is here applied at each point $x \in \Omega$ independently, hence, the output $[\mathcal{F}(u,\xi)](x,t)$ depends on $u(x,\cdot)|_{[0,t]}$, but not on $u(y,\cdot)|_{[0,t]}$ for $y \neq x$.

Remark 1 *Recall that the "initial state" ξ contains the "history" information needed to compute $\mathcal{F}$.*

We conclude by summarizing some properties that will be useful in the following sections. In particular, given an "initial state" ξ, $\mathcal{F}$ can be:

- *Causal*

$$\forall v_1, v_2 \in \mathcal{M}(\Omega; C([0,T])), \text{ if } v_1 = v_2 \quad \text{in } [0,t] \text{ a.e. in } \Omega,$$
$$\text{then } [\mathcal{F}(v_1, \xi)](\cdot, t) = [\mathcal{F}(v_2, \xi)](\cdot, t) \quad \forall t \in [0,T], \text{ a.e. in } \Omega. \tag{3.4}$$

- *Strongly continuous*

$$\forall \{v_n \in \mathcal{M}(\Omega; C([0,T]))\}_{n \in \mathbb{N}}, \text{if } v_n \to v \text{ uniformly in } [0,T] \text{ a.e. in } \Omega,$$
$$\text{then } \mathcal{F}(v_n, \xi) \to \mathcal{F}(v, \xi) \text{ uniformly in } [0,T] \quad \text{a.e. in } \Omega. \tag{3.5}$$

- *Piecewise monotone*

$$\forall v \in \mathcal{M}(\Omega; C([0,T])), \forall [t_1, t_2] \subset [0,T],$$
$$\text{if } v(x, \cdot) \text{ is affine in } [t_1, t_2] \text{ a.e. in } \Omega, \text{ then}$$
$$([\mathcal{F}(v, \xi)](x, t_2) - [\mathcal{F}(v, \xi)](x, t_1)) (v(x, t_2) - v(x, t_1)) \geq 0 \quad \text{a.e. in } \Omega. \tag{3.6}$$

7

4 The Preisach scalar hysteresis model

Different models have been proposed to represent the magnetic hysteresis phenomenon. At the macroscopic level, the most popular is the classical Preisach model [24]. This model is based on some hypotheses concerning the physical mechanisms of magnetization, and for this reason was primarily known in the area of magnetics. Nowadays it is recognized as a fundamental tool for describing a wide range of hysteresis phenomena in different subjects as electromagnetism and mechanics, among others. As mentioned in the introduction, in this section we briefly recall the classical definition and some properties of this operator following the works of Mayergoyz and Visintin (see [20, 34]).

4.1 Mathematical definition and properties

The classical Preisach model is constructed from an infinite set of hysteresis operators called *relay operators*. A relay operator is represented by elementary rectangular loops with "up" and "down" switching values. Given any couple $\rho = (\rho_1, \rho_2) \in \mathbb{R}^2$, with $\rho_1 < \rho_2$, the corresponding relay operator h_ρ, depicted in Figure 5, is defined as follows: for any $u \in C([0,T])$ and $\xi \in \{1, -1\}$, $h_\rho(u, \xi)$ is a function from $[0,T]$ to $\mathbb{R}$ such that,

$$h_\rho(u, \xi)(0) := \begin{cases} -1 & \text{if } u(0) \leq \rho_1, \\ \xi & \text{if } \rho_1 < u(0) < \rho_2, \\ 1 & \text{if } u(0) \geq \rho_2. \end{cases}$$
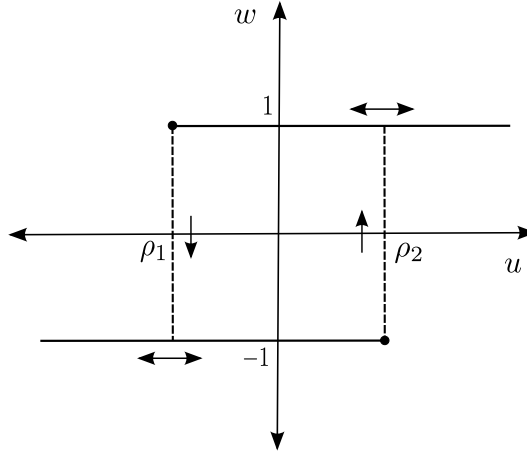

Figure 5: Scalar relay.

Then, for any $t \in (0,T]$, let us set $X_u(t) := \{\tau \in (0,t] : u(\tau) \in \{\rho_1, \rho_2\}\}$ and define

$$h_\rho(u, \xi)(t) := \begin{cases} h_\rho(u, \xi)(0) & \text{if } X_u(t) = \emptyset, \\ -1 & \text{if } X_u(t) \neq \emptyset \text{ and } u(\max X_u(t)) = \rho_1, \\ 1 & \text{if } X_u(t) \neq \emptyset \text{ and } u(\max X_u(t)) = \rho_2. \end{cases}$$

We notice that $h_\rho = \pm 1$ with "switch-up" and "switch-down" values at ρ_2 and ρ_1, respectively. The value of the relay operator remains at the last value (± 1) until u takes the value of one opposite switch, that is, switch to value $+1$ when u attains the value ρ_2 from below, and to -1 when it attains ρ_1 from above. This operator is the simplest model of discontinuous hysteresis.

Now, given $\rho_0 > 0$, let us introduce the *Preisach triangle* $\mathcal{T} := \{\rho = (\rho_1, \rho_2) \in \mathbb{R}^2 : -\rho_0 \leq \rho_1 \leq \rho_2 \leq \rho_0\}$ (see Figure 6 (left)). Let us denote by Y the family of Borel measurable functions $\mathcal{T} \to \{-1, 1\}$ and by ξ a generic element of Y. Let us define the Preisach operator

$$\widetilde{\mathcal{F}} : C([0, T]) \times Y \longrightarrow C([0, T]),$$

$$(u, \xi) \longmapsto [\widetilde{\mathcal{F}}(u, \xi)](t) = \int_{\mathcal{T}} [h_\rho(u, \xi(\rho))](t) p(\rho) \, d\rho, \qquad (4.7)$$

where $p \in \mathrm{L}^1(\mathcal{T})$ with $p > 0$ is known as the *Preisach function*. The Preisach model can be understood as the "sum" of a family of relays, distributed with a certain density p.

From the above definition of the hysteresis operator and [34, Theorems 1.2 and 3.2] we have the following result:

Lemma 1 *Given $\xi \in Y$, the Preisach operador $\widetilde{\mathcal{F}}(\cdot, \xi) : C([0, T]) \to C([0, T])$ is a hysteresis operator, strongly continuous and piecewise monotone. Moreover*

$$\left| [\widetilde{\mathcal{F}}(u, \xi)](t) \right| \leq \int_{\mathcal{T}} p(\rho) \, d\rho \qquad \forall u \in C([0, T]).$$

As in Section 3.2 it is possible to define the operator $\mathcal{F} : \mathcal{M}(\Omega; C([0, T]) \times Y) \to \mathcal{M}(\Omega; C([0, T]))$ as follows: given $(u, \xi) \in \mathcal{M}(\Omega; C([0, T]) \times Y)$

$$[\mathcal{F}(u, \xi)](r, z, t) := [\widetilde{\mathcal{F}}(u(r, z), \xi(r, z))](t) \qquad \forall t \in [0, T], \text{ a.e. in } \Omega. \qquad (4.8)$$

Then, by using similar results as those stated in Propositions 3.1 and 3.2 from [34, Section XII.3], adapted to the case of weighted Sobolev spaces, we can prove the following one:

Lemma 2 *Let $\xi : \Omega \to Y$ be an "initial state". Then, the operator $\mathcal{F}(\cdot, \xi) : \mathrm{L}^2_r(\Omega; C(0, T)) \to \mathrm{L}^2_r(\Omega; C(0, T))$ is causal, strongly continuous, piecewise monotone and affinely bounded (cf. (3.4), (3.5), (3.6) and (6.42), respectively).*

4.2 Geometric interpretation

The understanding of the Preisach operator is considerably facilitated by its geometric interpretation. This interpretation is based on the fact that there is a one-to-one correspondence between relay operators h_ρ and points (ρ_1, ρ_2) of the Preisach triangle $\mathcal{T}$.

We notice that, given $u \in C([0, T])$ and ξ, each relay $h_\rho(u, \xi(\rho))$ is such that, for any $t \in [0, T]$,

$$h_\rho(u, \xi(\rho))(t) := \begin{cases} 1 & \text{if } u(t) \leq \rho_1, \\ -1 & \text{if } u(t) \geq \rho_2, \\ \pm 1 & \text{if } \rho_2 < u(t) < \rho_1, \end{cases} \qquad (4.9)$$

and the choice of the sign above depends on $u|_{[0,t]}$ and $\xi(\rho)$. Therefore, for a given $u(t)$, all the relays h_ρ such that $\rho_1 \geq u(t)$ are "switched down". Similarly the relays h_ρ such that $\rho_2 \leq u(t)$ are "switched up" (see Figure 6 (right)).
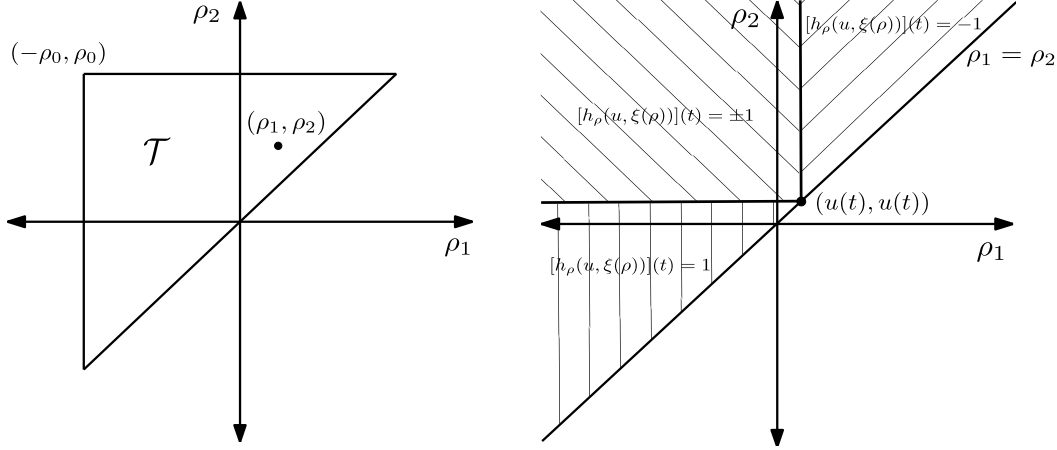
Figure 6: Preisach triangle (left) and Preisach domain (right).

Now, to understand the geometrical interpretation of the Preisach operator, we consider a simple setting and proceed in the same way as described by Mayergoyz in [20]. First we consider a function $u(t) \in C([0, T])$ as that shown in Figure 7 such that at some time t^0, $u(t^0) < -\rho_0$. Notice that, because of this particular choice of u, all the relays are well defined in $\mathcal{T}$ for $t > t^0$ without the need of giving an "initial state" ξ. Therefore, to simplify the notation, from now on, we drop out ξ and write $[h_\rho(u)](t) := [h_\rho(u, \xi)](t)$. Given that, $u(t^0) \leq -\rho_0 \leq \rho_1$ for all $(\rho_1, \rho_2) \in \mathcal{T}$, then from (4.9) it follows that all the relay operators $[h_\rho(u)](t^0) = -1$ in $\mathcal{T}$. Now, since u increases monotonically for $t \in [t^0, t^1]$, from the definition of the relay operator, the relays will only change to a positive state. Thus, at each time $t \geq t^0$, triangle $\mathcal{T}$ is subdivided into two sets (one possibly empty):

$$S_u^-(t) = \{(\rho_1, \rho_2) \in \mathcal{T} : [h_\rho(u)](t) = -1\} \quad \text{and} \quad S_u^+(t) = \{(\rho_1, \rho_2) \in \mathcal{T} : [h_\rho(u)](t) = 1\}.$$
(4.10)

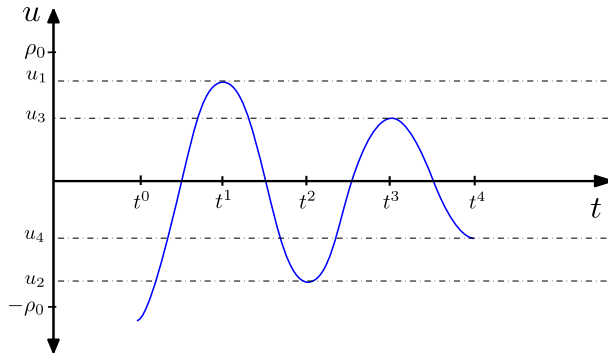Figure 7: Continuous function u.

Since the change to a positive state of the relay h_ρ depends only on the value of ρ_2, we obtain that the interface $L_u(t)$ between these two subsets is the line $\rho_2 = u(t)$ (see Figure 8 (left)) which moves up as u increases in time. Function u increases until it reaches some maximum value u_1 ($-\rho_0 < u_1 < \rho_0$) at time t^1 (see Figure 7)
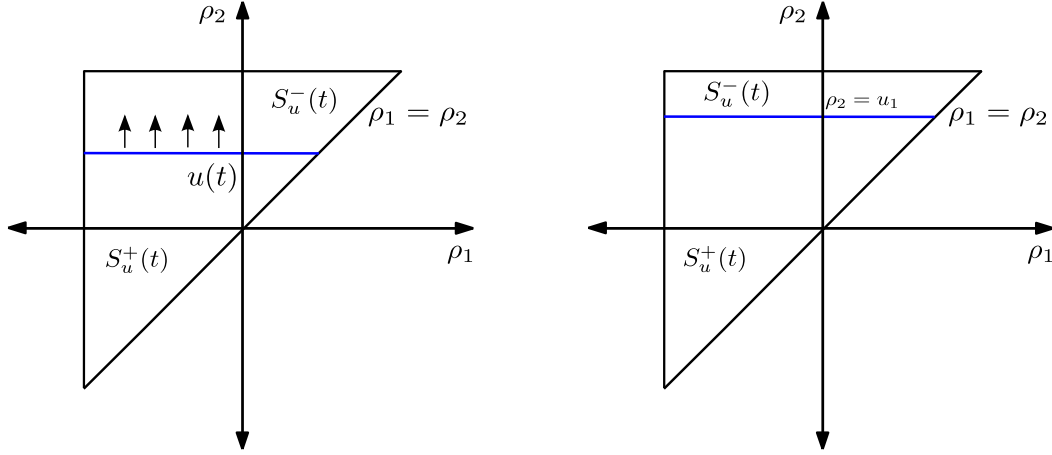
Figure 8: $L_u(t)$: $u(t)$ is increasing (left) and attains a maximum at u_1 (right).

Next, $u(t)$ decreases monotonically for $t \in [t^1, t^2]$. Then, the relays will only change to a negative state. Since changing to a negative state of the relay h_ρ depends only on the value of ρ_1, we obtain that the line $\rho_1 = u(t)$ moves from right to left (see Figure 9 (left)). Function u decreases until it reaches, at time t^2, some value $u_2 > -\rho_0$. At this point, the interface $L_u(t)$ between $S_u^+(t)$ and $S_u^-(t)$ has now two segments, the horizontal and vertical ones depicted in Figure 9 (right).
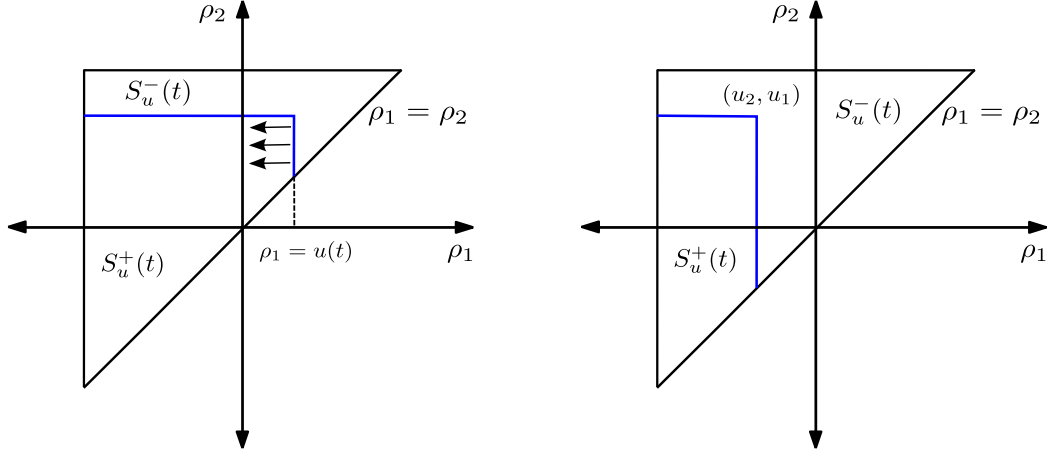

Figure 9: $L_u(t)$: $u(t)$ is decreasing from u_1 (left) and attains a minimum at u_2 (right).

Next, $u(t)$ increases again until it reaches at time t^3 some maximum value $u_3 < u_1$. Geometrically, this increment produces a new horizontal segment in $L_u(t)$ which moves up. This motion ends when the maximum u_3 is reached. This is shown in Figure 10 (left). Finally $u(t)$ decreases until it reaches, at time t^4, some minimum value $u_4 > u_2$. This variation results in a new vertical segment in $L_u(t)$ that moves from right to left as it is shown in Figure 10 (right). As shown in this figure, at this point, $L_u(t)$ has two vertices (u_2, u_1) and (u_4, u_3).
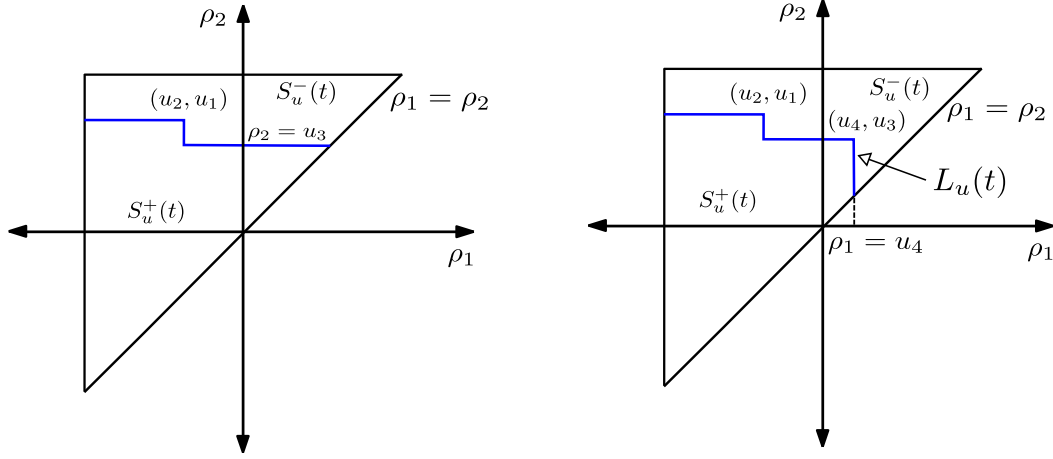
11

Figure 10: $L_u(t)$: $u(t)$ attains a maximum at u_3 (left) and attains a minimum at u_4 (right).

Remark 2 *A similar figure is obtained if we consider another function $v \in C([0,T])$ such that, at some time t^0, $v(t^0) > \rho_0$. We assume that $v(t)$ decreases to $v_1 > -\rho_0$, then increases to $v_2 \leq \rho_0$, next decreases to $v_3 > v_1$ and finally increases to $v_4 < v_2$, as depicted in Figure 11 (right). $L_v(t)$ is illustrated in Figure 11 (left).*
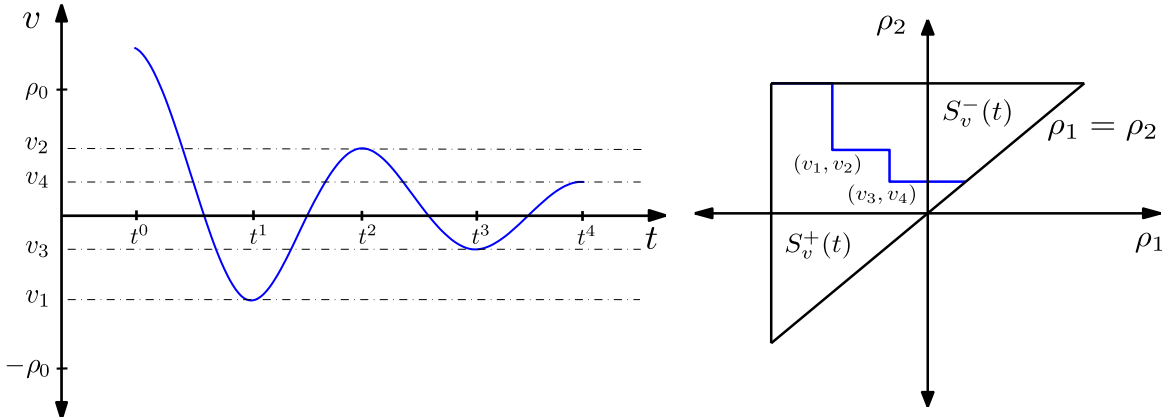

Figure 11: Staircase line $L_v(t)$ (left) and input $v(t)$ (right).

We can summarize the above analysis as follows; for a given $u \in C([0,T])$ as the one shown in Figure 7 and any time t, the triangle $\mathcal{T}$ is subdivided into two sets: $S_u^+(t)$ consisting of points (ρ_1, ρ_2) for which the corresponding relay operators $h_\rho(u)$ are positive, and $S_u^-(t)$ consisting of points (ρ_1, ρ_2) for which the corresponding relay operators $h_\rho(u)$ are negative. The interface $L_u(t)$ between $S_u^+(t)$ and $S_u^-(t)$ is a staircase line whose vertices have coordinates (ρ_1, ρ_2) coinciding respectively with the local minimum and maximum values of u at previous instants of time. At time t, the staircase line $L_u(t)$ intersects the line $\rho_1 = \rho_2$ at $(u(t), u(t))$. $L_u(t)$ moves up as $u(t)$ increases and it moves from right to left as $u(t)$ decreases (see Figure 12).
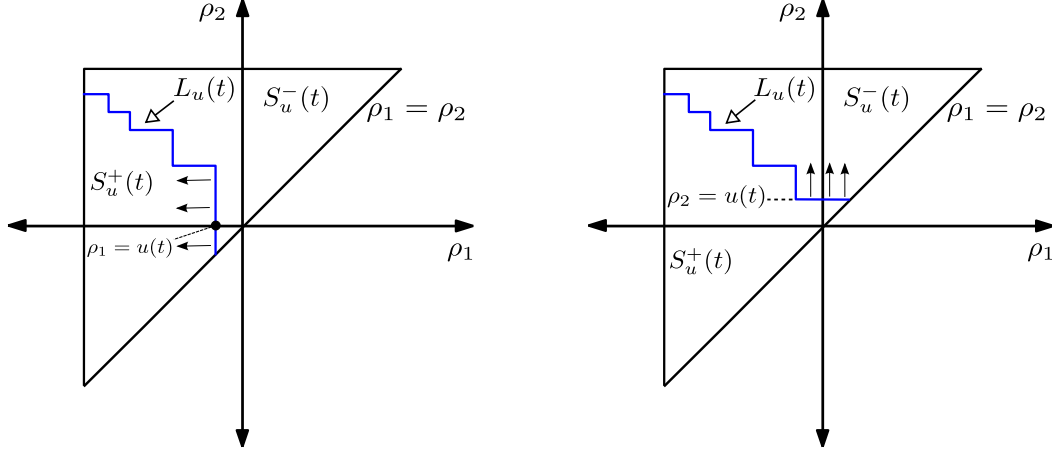
12

Figure 12: Staircase line $L_u(t)$ moving right to left (left) and moving up (right).

Hence, from the latter we notice that, at any time t, the integral in (4.7) can be subdivided into two integrals, over $S_u^+(t)$ and $S_u^-(t)$, respectively:

$$w_u(t) := [\widetilde{\mathcal{F}}(u)](t) = \int_{\mathcal{T}} [h_\rho(u)](t)p(\rho)\,d\rho$$
$$= \int_{S_u^+(t)} [h_\rho(u)](t)p(\rho)\,d\rho + \int_{S_u^-(t)} [h_\rho(u)](t)p(\rho)\,d\rho.$$

(We recall that, because of the particular choice of the values of u we do not need an "initial state" ξ.) Moreover, because of (4.10) and the latter equality we obtain that

$$w_u(t) = \int_{S_u^+(t)} p(\rho)\,d\rho - \int_{S_u^-(t)} p(\rho)\,d\rho. \tag{4.11}$$

Remark 3 *To compute the Preisach model in $(t^0, T]$, in general it is enough to know $u(t^0)$, the Preisach function p and the history of u represented by $S_u^+(t)$ and $S_u^-(t)$, which contain the least amount of information to compute (4.11).*

From (4.11), it follows that $[\widetilde{\mathcal{F}}(u)](t)$ depends on the particular subdivision of the limiting triangle $\mathcal{T}$ into $S_u^+(t)$ and $S_u^-(t)$. Therefore, it depends on the shape of the interface $L_u(t)$, which in its turn is determined by the extremum values of $u(t)$ at previous time. It turns out that not all extremal input values needed. In fact, given the dependence of the staircase line $L_u(t)$, we can see that the Preisach operator has a *wiping-out property*. This property states that each time the input reaches a local maximum $u(t)$, $L_u(t)$ erases, or "wipes out" the previous vertices of the staircase whose ρ_2 value is lower than the value $u(t)$. Similarly, each time an input reaches a local minimum $u(t)$, the memory curve erases all previous vertices whose ρ_1 value is higher than the $u(t)$ value.

To illustrate this property, we consider a simple setting. Let $u \in C([0,T])$ be characterized by a finite decreasing sequence $\{u_1, u_3, u_5, u_7\}$ of local maxima and an increasing sequence $\{u_2, u_4, u_6, u_8\}$ of local minima, with $-\rho_0 < u_i < \rho_0$, $i = 1, \ldots, 8$ (see Figure 13). Now, let us assume that $u(t)$ is monotonically increasing until it reaches u_9, such that $u_3 < u_9 < u_1$. This increase of $u(t)$ results in the formation of a new line in $L_u(t)$ which intersects the line $\rho_1 = \rho_2$ horizontally and moves up until the maximum value u_9 is reached. Then we obtain a modified staircase line $L_u(t)$ where all vertices whose ρ_2-coordinates are below u_9 have been wiped out (see Figure 14).

13
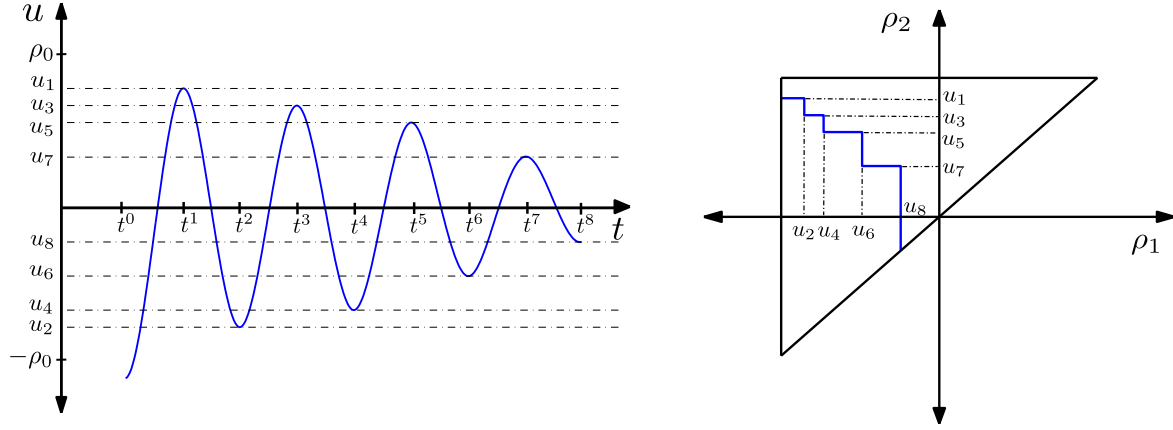
Figure 13: Function u (left) and initial staircase line L_u (right).
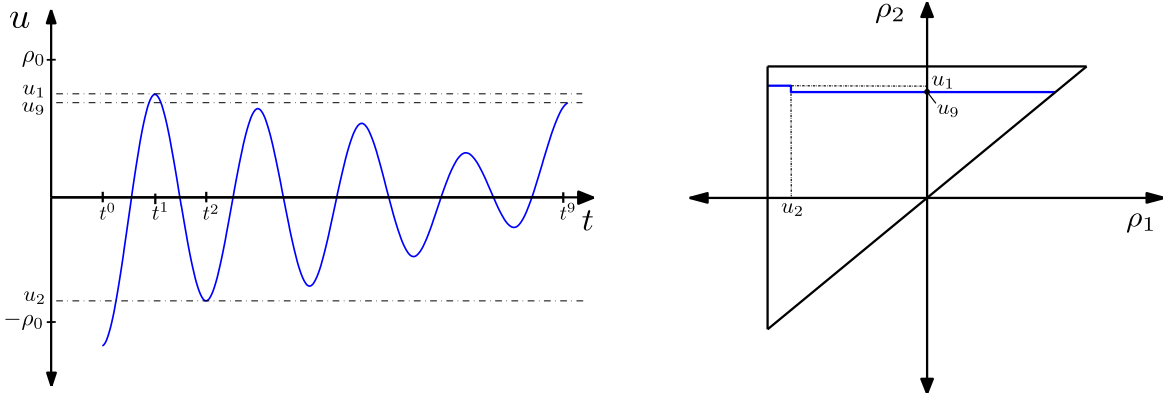
Figure 14: Function u (left) and L_u for increasing u until u_9 (right).

Similarly, instead of assuming that $u(t)$ is monotonically increasing, let us suppose that it decreases until it reaches u_9, such that $u_2 < u_9 < u_4$. Function u and the corresponding staircase line $L_u(t)$ are depicted in Figure 15.
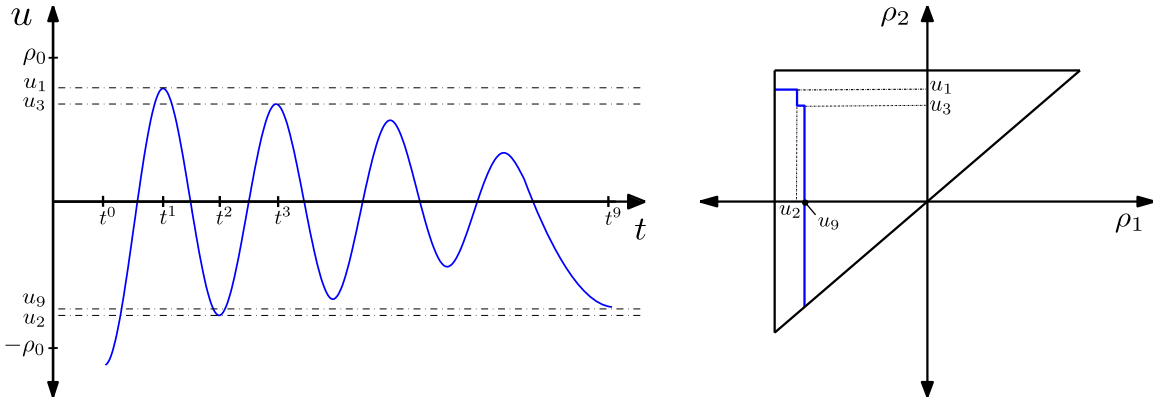
Figure 15: Function u (left) and L_u for decreasing u until u_9 (right).

Another important property of the Preisach operator is referred to as the *congruency property*. This property states that, as the input is cycled between two extremum values,

14

the minor loop traced will have the same shape, independently of history. However, the position of the minor loop along the output axis will be determined by the history of past input variations (see Figure 16, for further details, see [20]).
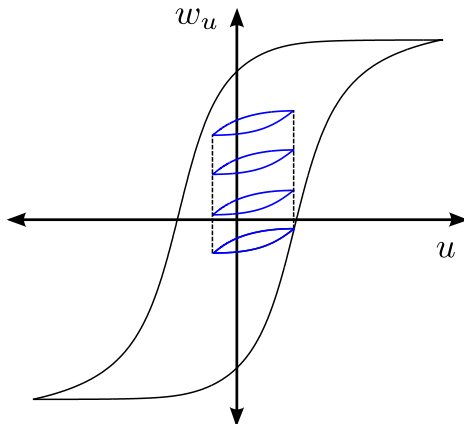
Figure 16: Congruency property.

4.3   Computation of the Preisach model

Once we have the distribution function and an "initial state", given $u \in C([0,T])$ we can compute $w_u(t) := [\widetilde{\mathcal{F}}(u)](t)$ by means of (4.7). Based on this feature, Mayergoyz [20] developed an approach for the computation of the Preisach model that does not require the Preisach function p but the so-called *Everett function* which describes the effect of p on the hysteresis operator. In what follows, for the sake of completeness, we describe the approach proposed by Mayergoyz in [20].

To obtain the Everett function, the so-called first order transition curves are required. To define such a curve, first we consider a function $u \in C([0,T])$, such that at time t^0, $u(t^0) \leq -\rho_0$. Then, u increases monotonically until it reaches some value ρ_2' at time t^1. We denote $w_{\rho_2'} := w_u(t^1)$. A first order transition curve is formed by the above monotonic increase of u followed by a subsequent monotonic decrease, namely, from ρ_2', u decreases monotonically until it reaches some value $\rho_1' < \rho_2'$ at time t^2; we denote $w_{\rho_2',\rho_1'} := w_u(t^2)$ (see Figures 18 and 17).
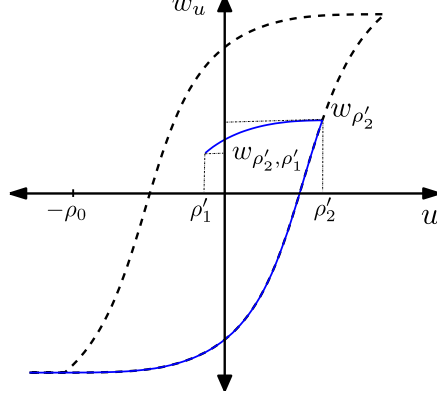
Figure 17: First order transition curve.
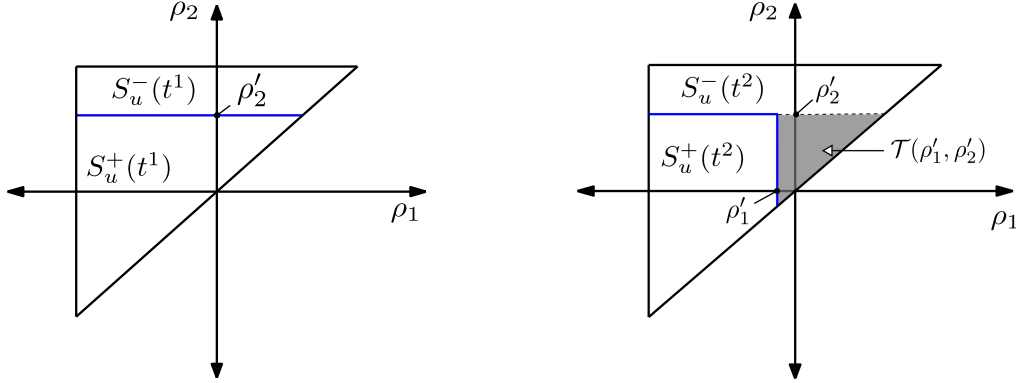
Figure 18: Staircase line $L_u(t)$ at time t^1 (left) and at time t^2 (right).

We define the Everett function $E : \mathcal{T} \to \mathbb{R}$ by

$$E(\rho_1', \rho_2') := \frac{w_{\rho_2'} - w_{\rho_2', \rho_1'}}{2}. \tag{4.12}$$

From (4.11), we notice that

$$w_{\rho_2', \rho_1'} - w_{\rho_2'} = \left(\int_{S_u^+(t^2)} p(\rho)\, d\rho - \int_{S_u^-(t^2)} p(\rho)\, d\rho \right) - \left(\int_{S_u^+(t^1)} p(\rho)\, d\rho - \int_{S_u^-(t^1)} p(\rho)\, d\rho \right)$$

$$= -2 \int_{\mathcal{T}(\rho_1', \rho_2')} p(\rho)\, d\rho,$$

with $\mathcal{T}(\rho_1', \rho_2')$ the triangle shown in Figure 18 (right) with the vertex of the right angle at (ρ_1', ρ_2'). This is so because $S_u^+(t^2) = S_u^+(t^1) \setminus \mathcal{T}(\rho_1', \rho_2')$ and $S_u^-(t^2) = S_u^-(t^1) \cup \mathcal{T}(\rho_1', \rho_2')$ (see Figure 18 (right)). Therefore, we obtain the following relation between the Preisach function p and the Everett function E:

$$E(\rho_1, \rho_2) = \int_{\mathcal{T}(\rho_1, \rho_2)} p(\rho)\, d\rho \qquad \forall (\rho_1, \rho_2) \in \mathcal{T}. \tag{4.13}$$

16

To take into account this relation in the computation of the Preisach operator, first we rewrite (4.11), by adding and subtracting the integral of p over $S_u^+(t)$ as follows:

$$w_u(t) = 2 \int_{S_u^+(t)} p(\rho)\, d\rho - \int_{\mathcal{T}} p(\rho)\, d\rho,$$

where $\mathcal{T}$ is the Preisach triangle. Moreover, from (4.13) and the definition of the Preisach triangle $\mathcal{T} = \mathcal{T}(-\rho_0, \rho_0)$ (cf. Figure 6 (left)) it follows that,

$$w_u(t) = 2 \int_{S_u^+(t)} p(\rho)\, d\rho - E(-\rho_0, \rho_0). \tag{4.14}$$

Provided that the Preisach function p is known, to obtain $w_u(t)$ we can compute the both terms on the right-hand side of (4.14). For this purpose we further assume that u is piecewise monotonic and distinguish two cases: u monotonically increasing and u monotonically decreasing in an interval (t', t) for some $t' < t$. For decreasing u, we subdivide $S_u^+(t)$ into n trapezoids $Q_k(t)$ (see Figure 19 (left)). We can perform this subdivision because, for decreasing arguments, the staircase line $L_u(t)$ intersects the line $\rho_1 = \rho_2$ vertically. Then we have

$$\int_{S_u^+(t)} p(\rho)\, d\rho = \sum_{k=1}^{n(t)} \int_{Q_k(t)} p(\rho)\, d\rho, \tag{4.15}$$

where $n(t)$ is the number of local maxima of u up to time t that have not been wiped-out (recall the wipe-out process as illustrated in Figure 15)
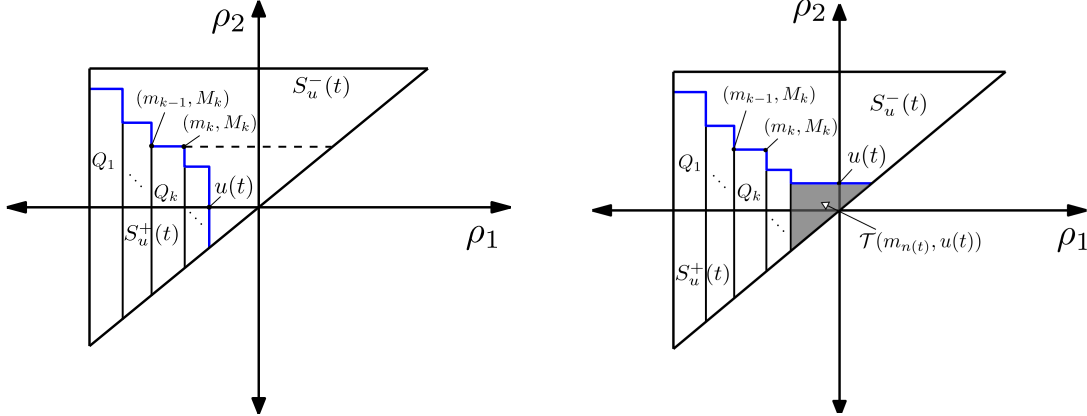
Figure 19: Staircase line for a decreasing input (left) and a increasing input (right).

Each trapezoid $Q_k(t)$ depends on the local maximum M_k and on the local minima m_k and m_{k-1}. Notice that, for $k = 1$, $m_0 = -\rho_0$. Moreover, each trapezoid can be represented as the set difference of two triangles $\mathcal{T}(m_{k-1}, M_k)$ and $\mathcal{T}(m_k, M_k)$:

$$\int_{Q_k(t)} p(\rho)\, d\rho = \int_{\mathcal{T}(m_{k-1}, M_k)} p(\rho)\, d\rho - \int_{\mathcal{T}(m_k, M_k)} p(\rho)\, d\rho. \tag{4.16}$$

Now, from (4.13), it follows that

$$\int_{S_u^+(t)} p(\rho)\, d\rho = \sum_{k=1}^{n(t)} \left(E(m_{k-1}, M_k) - E(m_k, M_k) \right). \tag{4.17}$$

17

Finally, from (4.17) and (4.14), we obtain

$$w_u(t) = 2 \sum_{k=1}^{n(t)} (E(m_{k-1}, M_k) - E(m_k, M_k)) - E(-\rho_0, \rho_0).$$

Since we consider u monotonically decreasing in (t', t), we obtain that the last minimum value $m_{n(t)}$ is equal to the current value of u, namely, $m_{n(t)} = u(t)$. Then

$$w_u(t) = -E(-\rho_0, \rho_0) + 2 \sum_{k=1}^{n(t)-1} (E(m_{k-1}, M_k) - E(m_k, M_k)) \tag{4.18}$$

$$+ 2 \left(E(m_{n(t)-1}, M_{n(t)}) - E(u(t), M_{n(t)}) \right). \tag{4.19}$$

Because of the decomposition of S_u^+ into trapezoids (see Figure 19), this expression is valid only for u being monotonically decreasing in (t', t). If $u(t)$ is monotonically increasing, then the staircase line $L_u(t)$ intersects the line $\rho_1 = \rho_2$ horizontally. Hence, we may decompose S_u^+ into trapezoids and a triangle (see Figure 19 (right)). It follows that

$$\int_{S_u^+(t)} p(\rho) \, d\rho = \sum_{k=1}^{n(t)-1} (E(m_{k-1}, M_k) - E(m_k, M_k)) + E(m_{n(t)-1}, M_{n(t)}). \tag{4.20}$$

In this case, the last maximum value $M_{n(t)}$ is equal to the current value of u, namely, $M_{n(t)} = u(t)$. Hence, from (4.20) we write (4.14) for a monotonically increasing u in (t', t) as follows:

$$w_u(t) = -E(-\rho_0, \rho_0) + 2 \sum_{k=1}^{n(t)-1} (E(m_{k-1}, M_k) - E(m_k, M_k)) + 2E(m_{n(t)-1}, u(t)). \tag{4.21}$$

From (4.18) and (4.21) we obtain the following expression to compute the Preisach operator in terms of the Everett function

$$w_u(t) := \begin{cases} -E(-\rho_0, \rho_0) + 2 \sum_{k=1}^{n(t)-1} (E(m_{k-1}, M_k) - E(m_k, M_k)) \\ \qquad + 2 \left(E(m_{n(t)-1}, M_{n(t)}) - E(u(t), M_{n(t)}) \right) \quad \text{for } u \text{ decreasing,} \\ \\ -E(-\rho_0, \rho_0) + 2 \sum_{k=1}^{n(t)-1} (E(m_{k-1}, M_k) - E(m_k, M_k)) \\ \qquad + 2E(m_{n(t)-1}, u(t)) \hspace{4cm} \text{for } u \text{ increasing.} \end{cases}$$

As an example, we compute $w_u(t)$ by using the Preisach function p given by the Factorized-Lorentzian distribution (see [6]):

$$p(\rho_1, \rho_2) := N \left(\left(1 + \left(\frac{\rho_2 - \omega}{\gamma \omega} \right)^2 \right) \left(1 + \left(\frac{\rho_1 + \omega}{\gamma \omega} \right)^2 \right) \right)^{-1} \tag{4.22}$$

with parameters $N = 1, \omega = 0.8$ and $\gamma = 0.6$ (see Figure 20). The Preisach triangle $\mathcal{T}$ is characterized by $\rho_0 = 5$.
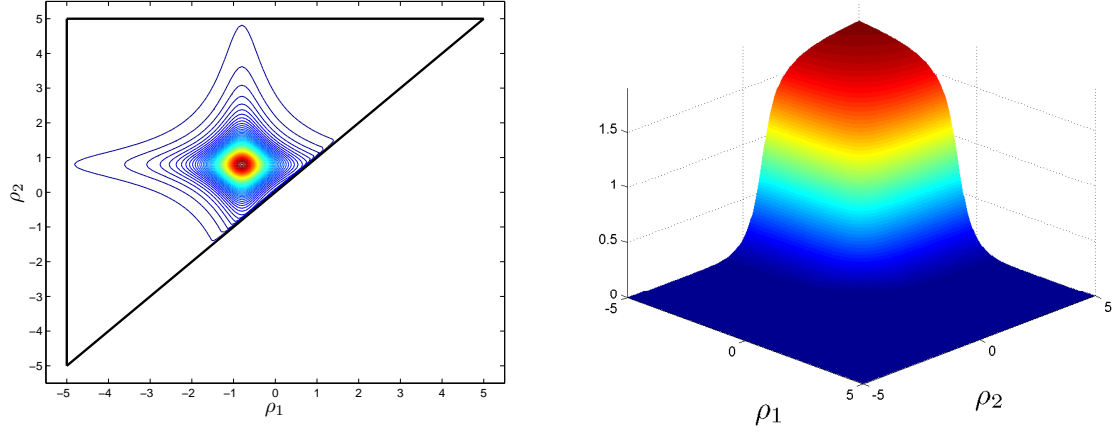
Figure 20: Factorized-Lorentzian distribution function p (left) and corresponding Everett function (right).

We compute the $w_u - u$ loop in two cases. First we consider the input function $u(t)$ shown in Figure 21. The evolution of the corresponding $w_u - u$ loop are shown in Figure 22 at times t^1, t^2, t^3 and t^4.
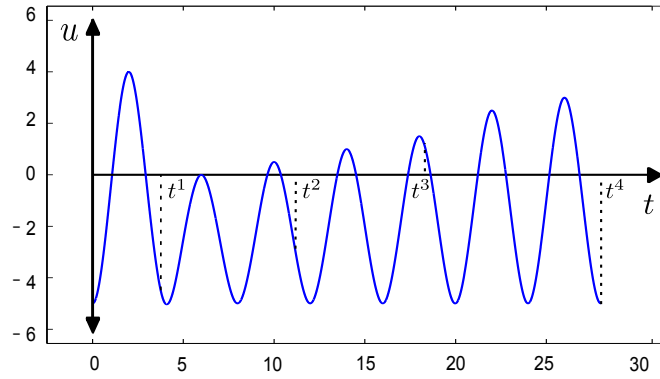
Figure 21: Function $u(t)$.
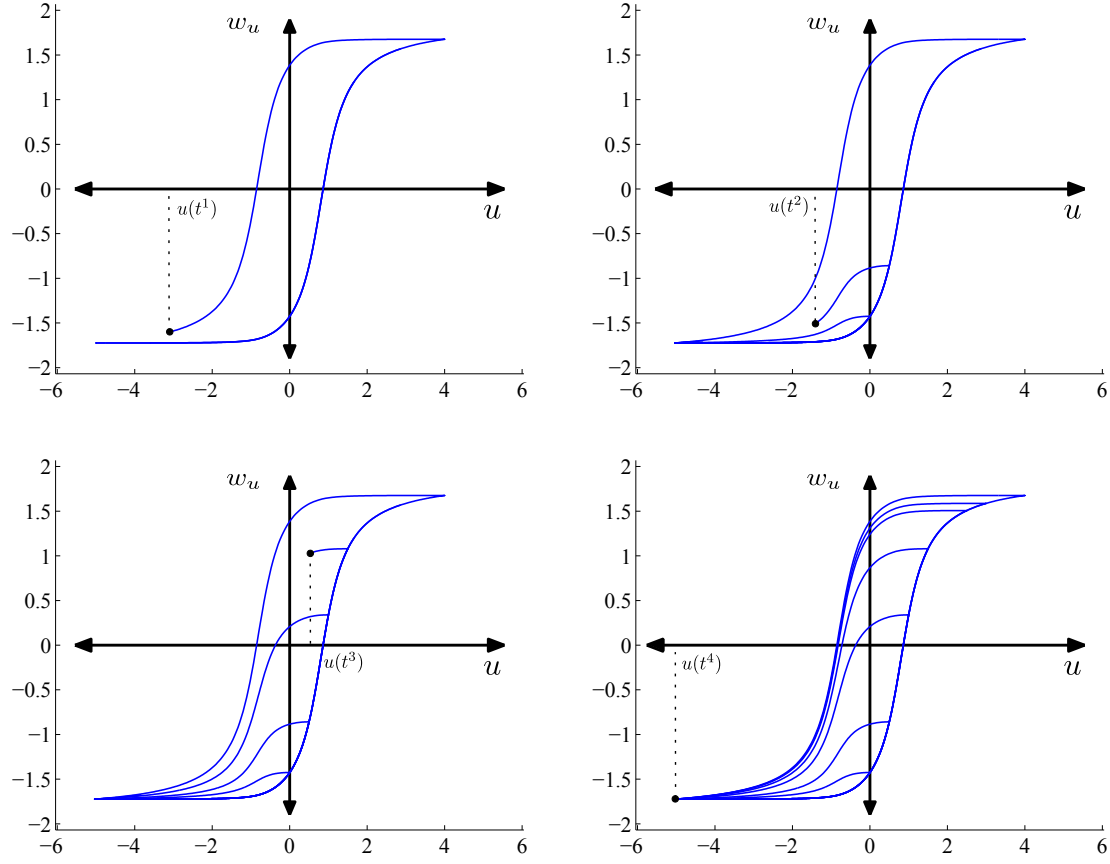
Figure 22: $w_u - u$ curve at time t^1, t^2, t^3 and t^4.

Finally we consider the input function $u(t)$ shown in Figure 23. In this case we present in Figure 24 the final staircase line and the complete $w_u - u$ loop.
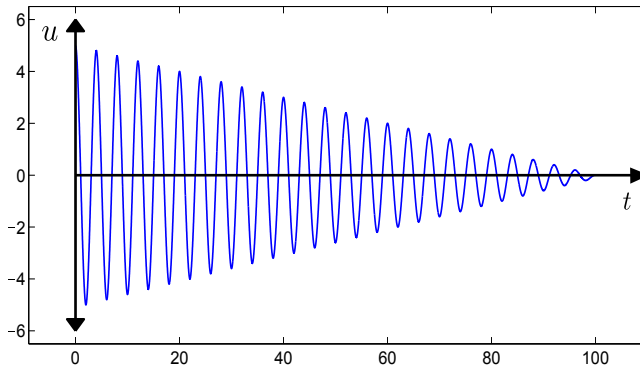
Figure 23: Function $u(t)$.
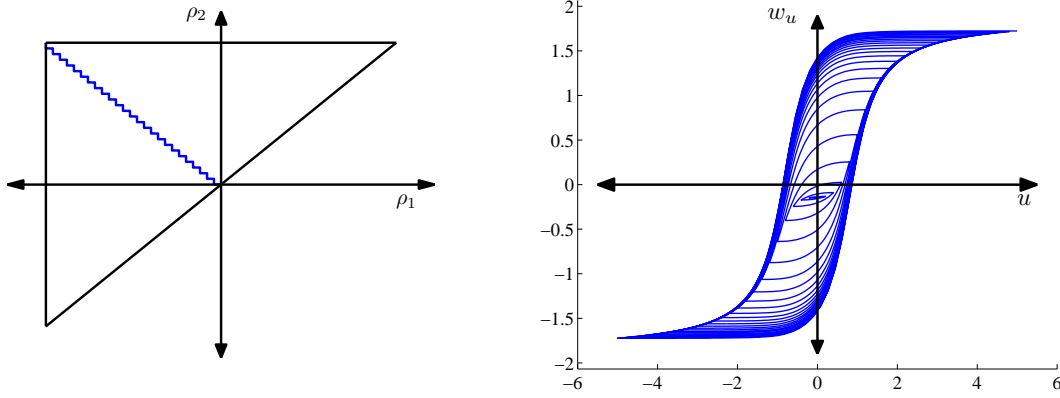
Figure 24: Staircase function (left) and $w_u - u$ curve (right).

Remark 4 *In the previous examples we consider different inputs u, such that $u(t^0) \geq \rho_0$ or $u(t^0) \leq -\rho_0$. Clearly, in both cases $S_u^+(t^0)$ and $S_u^-(t^0)$ are determined and because of that, there is not need to consider additional information to compute $w_u(t)$, $t \geq t^0$. In particular, we have $w_u(t^0) = E(-\rho_0, \rho_0)$ if $u(t^0) \geq \rho_0$, and $-E(-\rho_0, \rho_0)$ if $u(t^0) \leq -\rho_0$. However, in the case of $-\rho_0 < u(t^0) < \rho_0$, to compute $w_u(t^0)$ we must have an "initial state". To illustrate this we consider three different previous "histories" of u as shown in the curves $u_1(t), u_2(t)$ and $u_3(t)$ in Figure 25. The curves u_1 and u_3 are extreme cases in which:*

$$u_1(t) \leq u_1(t^0) = u_0 \qquad \forall t \leq t^0$$
$$u_3(t) \geq u_3(t^0) = u_0 \qquad \forall t \leq t^0.$$

Instead, u_2 takes values large and smaller that u_0 for $t < t^0$.
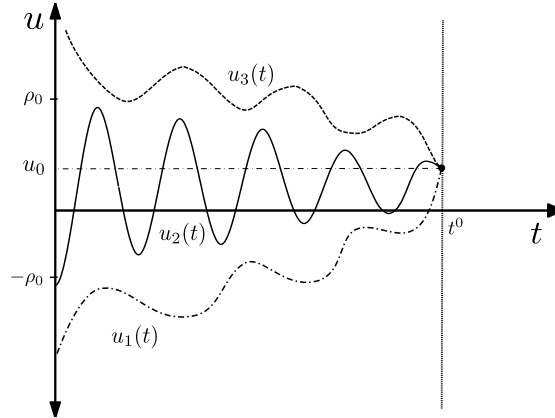
Figure 25: Functions $u_1(t), u_2(t)$ and $u_3(t)$.

We show in Figure 26 (left) the corresponding staircase lines L_{u_1}, L_{u_2} and L_{u_3} and in Figure 26 (right) the corresponding values of $w_u(u_1)$, $w_u(u_2)$ and $w_u(u_3)$ at time $t = t^0$ (w_u^1, w_u^2 and w_u^3, respectively). Notice that the three values are different; w_u^1 and w_u^3 lie on the major loop, whereas w_u^2 lies in the interval (w_u^1, w_u^3).
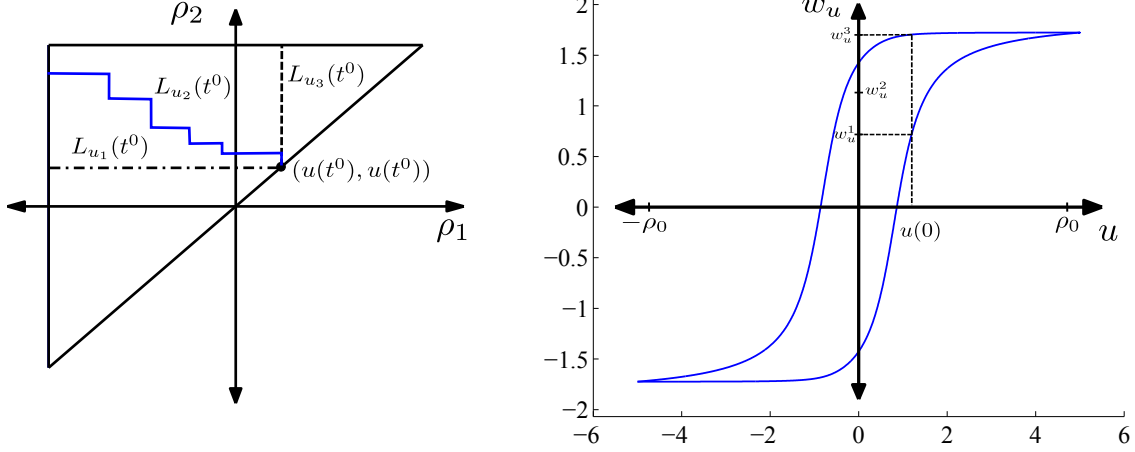
Figure 26: Staircase function (left) $w_u - u$ curve (right).

In what follows, we will take into account the previous discussion to study a particular transient eddy current problem where hysteresis effects are considered.

5   The transient eddy current model with hysteresis

Eddy currents are modeled by the so-called low-frequency Maxwell's equations:

$$
\begin{aligned}
\mathbf{curl}\,\boldsymbol{H} &= \boldsymbol{J}, \\
\frac{\partial \boldsymbol{B}}{\partial t} + \mathbf{curl}\,\boldsymbol{E} &= \boldsymbol{0}, \\
\mathrm{div}\,\boldsymbol{B} &= 0,
\end{aligned}
$$

where we have used the standard notation in electromagnetism: $\boldsymbol{E}$ is the electric field, $\boldsymbol{B}$ the magnetic induction, $\boldsymbol{H}$ the magnetic field and $\boldsymbol{J}$ the current density.

In order to obtain a closed system we need constitutive laws. We have the Ohm's law in conductors,

$$
\boldsymbol{J} = \sigma \boldsymbol{E},
$$

where σ is the electrical conductivity and we consider the constitutive equation

$$
\boldsymbol{B} = \mu_0 \left(\boldsymbol{H} + \boldsymbol{M} \right),
$$

where $\boldsymbol{M}$ is the magnetization and μ_0 is the magnetic permeatibity of the vacuum. In ferromagnetic and ferrimagnetic materials, where hysteresis phenomena may occur, the dependence between $\boldsymbol{M}$ and $\boldsymbol{H}$ exhibits a history-dependent behavior and must be represented by a suitable constitutive law accounting for hysteresis. We synthetically represent this dependence in the form

$$
\boldsymbol{M} = \boldsymbol{\mathcal{F}}(\boldsymbol{H}),
$$

where $\boldsymbol{\mathcal{F}}$ is a vector *hysteresis operator* (see [21, 20]). This dependence is nonlocal in time but pointwise in space. We notice that a real ferromagnetic material may exhibit rate dependent memory effects but they will not be considered in this analysis.

From the above equations we can easily obtain the following vector partial differential equation in conductors:

$$
\frac{\partial \boldsymbol{B}}{\partial t} + \mathbf{curl} \left(\frac{1}{\sigma} \mathbf{curl}\,\boldsymbol{H} \right) = \boldsymbol{0}, \tag{5.23}
$$

22

which has to be solved together the constitutive equation

$$\boldsymbol{B} = \mu_0 \left(\boldsymbol{H} + \boldsymbol{\mathcal{F}}(\boldsymbol{H}) \right) \tag{5.24}$$

in a conducting domain $\widetilde{\Omega} \subset \mathbb{R}^3$.

5.1 Axisymmetric eddy current model

In many applications the computational domain $\widetilde{\Omega}$ has cylindrical symmetry and all fields are independent of the angular variable θ. In such a case, in order to reduce the dimension and thereby the computational effort, it is convenient to consider a cylindrical coordinate system (r, θ, z). Let us denote by $\mathbf{e}_r$, $\mathbf{e}_\theta$ and $\mathbf{e}_z$ the corresponding unit vectors of the local orthonormal basis.

Moreover, let us assume the magnetic field has only azimuthal component, i.e., it is of the form,

$$\boldsymbol{H}(r, z, t) = H(r, z, t)\mathbf{e}_\theta. \tag{5.25}$$

If we also assume that the materials composing the domain have an isotropic behavior, then $\boldsymbol{B}$ has only azimuthal component too:

$$\boldsymbol{B}(r, z, t) = B(r, z, t)\mathbf{e}_\theta. \tag{5.26}$$

We notice that any field of the form (5.26) is divergence–free.

According to (5.25),

$$\mathbf{curl}\, \boldsymbol{H}(r, z, t) = -\frac{\partial}{\partial z} H(r, z, t)\mathbf{e}_\theta + \frac{1}{r}\frac{\partial}{\partial r}(rH)(r, z, t)\mathbf{e}_z, \tag{5.27}$$

and then equation (5.23) reads

$$\frac{\partial B}{\partial t} - \frac{\partial}{\partial r}\left(\frac{1}{\sigma r}\frac{\partial(rH)}{\partial r} \right) - \frac{\partial}{\partial z}\left(\frac{1}{\sigma}\frac{\partial H}{\partial z} \right) = 0.$$

This equation holds in a meridian section Ω of $\widetilde{\Omega}$, for all time $t \in [0, T]$.

In order to write a well-posed problem we must add an initial condition

$$B(r, z, 0) = B_0(r, z) \quad \text{in } \Omega, \tag{5.28}$$

and appropriate source terms. In view of applications, we will consider alternatively the two following cases:

- Non-homogeneous Dirichlet condition:

$$H(r, z, t) = g(r, z, t) \qquad \text{on } \Gamma,$$

where g is a given function and $\Gamma := \partial\Omega$. For applications of this model, we refer for instance to [1, 2, 17], where a Dirichlet problem arises in the simulation of metallurgical electrodes, or the computation of current losses in a toroidal laminated core [19, 22]. In this case, the Dirichlet boundary data g can be obtained from the current intensity.

- Magnetic flux condition:

$$\int_\Omega B(r, z, t)\, drdz = b(t), \tag{5.29}$$

$$rH|_\Gamma = \psi(t) \qquad \text{on } \Gamma, \tag{5.30}$$

where b is a given function but ψ is unknown; the meaning of the last condition is just that at each time t, rH is constant on Γ. The above integral in (5.29) represents the magnetic flux $b(t)$ through a meridian section Ω of the domain. Such a condition holds, for instance, in toroidal transformers when a voltage drop between the ends of the coil is applied (see, for instance, [28]).

Finally, taking into account that the involved fields are scalar, relation (5.24) can be described as

$$B(r, z, t) = \mu_0 \left(H(r, z, t) + [\mathcal{F}(H)](r, z, t) \right), \tag{5.31}$$

where $\mathcal{F}$ is a scalar hysteresis operator.

All together, the two resulting axisymmetric problems read:

Problem 5.1 *Find $H_D(r, z, t)$ and $B_D(r, z, t)$ such that*

$$\frac{\partial B_D}{\partial t} - \frac{\partial}{\partial r} \left(\frac{1}{\sigma r} \frac{\partial (r H_D)}{\partial r} \right) - \frac{\partial}{\partial z} \left(\frac{1}{\sigma} \frac{\partial H_D}{\partial z} \right) = f \quad in \ \Omega \times (0, T), \tag{5.32}$$

$$B_D = \mu_0 \left(H_D + \mathcal{F}(H_D, \xi) \right) \quad in \ \Omega \times (0, T), \tag{5.33}$$

$$H_D = g \quad on \ \Gamma \times (0, T), \tag{5.34}$$

$$B_D|_{t=0} = B_{D0} \quad in \ \Omega. \tag{5.35}$$

Problem 5.2 *Find $H_N(r, z, t)$, $B_N(r, z, t)$ and $\psi(t)$ such that*

$$\frac{\partial B_N}{\partial t} - \frac{\partial}{\partial r} \left(\frac{1}{\sigma r} \frac{\partial (r H_N)}{\partial r} \right) - \frac{\partial}{\partial z} \left(\frac{1}{\sigma} \frac{\partial H_N}{\partial z} \right) = f \quad in \ \Omega \times (0, T), \tag{5.36}$$

$$B_N = \mu_0 \left(H_N + \mathcal{F}(H_N, \xi) \right) \quad in \ \Omega \times (0, T), \tag{5.37}$$

$$r H_N(r, z, t) = \psi(t) \quad on \ \Gamma \times (0, T), \tag{5.38}$$

$$\int_\Omega B_N(r, z, t) \, dr dz = b(t) \quad in \ (0, T), \tag{5.39}$$

$$B_N|_{t=0} = B_{N0} \quad in \ \Omega. \tag{5.40}$$

In the problems above $\sigma(r, z, t), f(r, z, t), g(r, z, t), b(t), \xi(r, z), B_{D0}(r, z)$ and $B_{N0}(r, z)$ are given functions.

Remark 5 *For the sake of completeness, in (5.32) and (5.36) we have considered a general right-hand side f. Moreover, we consider a space and time dependent electrical conductivity σ because, in practical applications, σ is a function of temperature which, in its turn, is a time dependent field.*

Remark 6 *Notice that, in order to compute the hysteresis operator $[\mathcal{F}(H)]$ a.e. in $\Omega \times [0, T]$, we need to provide an appropriate "initial state" (cf. Remark 1). From a practical point of view, a typical initial condition (cf. (5.35) and (5.40)) is the so-called demagnetized or virginal state of the material, namely, $(B, H)|_{t=0} = (0, 0)$. The demagnetized state can be achieved, for instance, by heating the material above its Curie temperature. Another method that returns the material to a nearly demagnetized state is to apply a magnetic field with a direction that changes back and forth, while at the same time its amplitude reduces to zero.*

6 Mathematical analysis

In this section, we derive weak formulations for Problems 5.1 and 5.2, and prove that they are well-posed. The techniques used for this purpose are based on [34, Chapter IX], where the existence of solution to a similar 2D problem in standard Sobolev spaces with homogeneous Dirichlet condition is proved (for a homogeneous Neumann condition we refer to [12, 31]).

The presence of time dependent coefficients, the different source terms (cf. (5.34) and (5.39)) and the fact that the problems are posed on weighted Sobolev spaces because of the cylindrical symmetry assumption brings some technical complications to the analysis with respect to previous works on the subject. In particular, (5.38)–(5.39) yield a non-classical boundary condition for the resulting non-linear parabolic problem. Such a condition and the fact of having a time dependent conductivity (cf. Remark 5), lead us to deal with a time dependent bilinear form which, instead of being elliptic, satisfies a Gårding's inequality. On the other hand, with respect to Problem 5.1, in order to deal with condition (5.34) we have to introduce a *lifting* of the boundary data which brings additional complications in the mathematical analysis.

First, we introduce some preliminary results.

6.1 Functional spaces and preliminary results

We define appropriate weighted Sobolev spaces that will be used for the mathematical analysis of the problem and recall some of their properties. For the sake of simplicity, in this paragraph the partial derivatives will be denoted by ∂_r and ∂_z.

Let $\Omega \subset \left\{ (r,z) \in \mathbb{R}^2 : r > 0 \right\}$ be a bounded connected two-dimensional open set with a connected Lipschitz boundary Γ. Let $\mathrm{L}_r^2(\Omega)$ denote the weighted Lebesgue space of all measurable functions u defined in Ω for which

$$\|u\|_{\mathrm{L}_r^2(\Omega)}^2 := \int_\Omega |u|^2 r \, drdz < \infty.$$

The weighted Sobolev space $\mathrm{H}_r^1(\Omega)$ consists of all functions in $\mathrm{L}_r^2(\Omega)$ whose first derivatives are also in $\mathrm{L}_r^2(\Omega)$. We define the norms and semi-norms in the standard way; in particular,

$$|u|_{\mathrm{H}_r^1(\Omega)}^2 := \int_\Omega \left(|\partial_r u|^2 + |\partial_z u|^2 \right) r \, drdz.$$

Let $\widetilde{\mathrm{H}}_r^1(\Omega) := \mathrm{H}_r^1(\Omega) \cap \mathrm{L}_{1/r}^2(\Omega)$, where $\mathrm{L}_{1/r}^2(\Omega)$ denotes the set of all measurable functions u defined in Ω for which

$$\|u\|_{\mathrm{L}_{1/r}^2(\Omega)}^2 := \int_\Omega \frac{|u|^2}{r} \, drdz < \infty.$$

$\widetilde{\mathrm{H}}_r^1(\Omega)$ is a Hilbert space with the norm

$$\|u\|_{\widetilde{\mathrm{H}}_r^1(\Omega)}^2 := \|u\|_{\mathrm{H}_r^1(\Omega)}^2 + \|u\|_{\mathrm{L}_{1/r}^2(\Omega)}^2 .$$

We recall from [15, Section 3] that functions in $\widetilde{\mathrm{H}}_r^1(\Omega)$ have traces on Γ. We denote

$$\widetilde{\mathrm{H}}_r^{1/2}(\Gamma) := \left\{ v|_\Gamma : v \in \widetilde{\mathrm{H}}_r^1(\Omega) \right\}$$

endowed with the norm

$$\|g\|_{\widetilde{\mathrm{H}}_r^{1/2}(\Gamma)} := \inf \left\{ \|v\|_{\widetilde{\mathrm{H}}_r^1(\Omega)} : v \in \widetilde{\mathrm{H}}_r^1(\Omega), v|_\Gamma = g \right\}$$

which makes the trace operator $v \to v|_\Gamma$ continuous.

Also, let us introduce the function space $\widehat{\mathrm{H}}_r^1(\Omega)$ defined by

$$\widehat{\mathrm{H}}_r^1(\Omega) := \left\{ u \in \mathrm{L}_r^2(\Omega) : \partial_r(ru) \in \mathrm{L}_{1/r}^2(\Omega), \partial_z u \in \mathrm{L}_r^2(\Omega) \right\}$$

which is a Hilbert space with the norm

$$\|u\|_{\widehat{\mathrm{H}}_r^1(\Omega)}^2 := \left(\|u\|_{\mathrm{L}_r^2(\Omega)}^2 + \|\partial_r(ru)\|_{\mathrm{L}_{1/r}^2(\Omega)}^2 + \|\partial_z u\|_{\mathrm{L}_r^2(\Omega)}^2 \right)^{1/2}.$$

Clearly $\widetilde{\mathrm{H}}_r^1(\Omega) \subset \widehat{\mathrm{H}}_r^1(\Omega)$.

Finally, given a Banach space Q, we introduce the space $\mathrm{L}_r^2(\Omega; Q)$ of all function $u : \Omega \to Q$ such that

$$\|u\|_{\mathrm{L}_r^2(\Omega;Q)}^2 := \int_\Omega \|u(r,z)\|_Q^2 \, r \, dr dz < \infty.$$

Remark 7 *For Ω being a meridian section of a 3D axisymmetric domain $\widetilde{\Omega}$, the space $\widehat{\mathrm{H}}_r^1(\Omega)$ can be considered as an axisymmetric version of the 3D space $\mathbf{H}(\mathbf{curl}, \widetilde{\Omega}) := \{ \mathbf{u} \in \mathrm{L}^2(\widetilde{\Omega})^3 : \mathbf{curl}\, \mathbf{u} \in \mathrm{L}^2(\widetilde{\Omega})^3 \}$. In fact, it is easy to see that $G(r,z) \in \widehat{\mathrm{H}}_r^1(\Omega)$ if and only if $\mathbf{G}(r,z,\theta) = G(r,z)\mathbf{e}_\theta(\theta) \in \mathbf{H}(\mathbf{curl}, \widetilde{\Omega})$. Similarly, we deduce that $G(r,z) \in \widetilde{\mathrm{H}}_r^1(\Omega)$ if and only if $\mathbf{G}(r,z,\theta) = G(r,z)\mathbf{e}_\theta(\theta) \in \mathrm{H}^1(\widetilde{\Omega})^3$.*

Moreover, given $\mathbf{G}$ of the form $\mathbf{G}(r,z,\theta) = G(r,z)\mathbf{e}_\theta(\theta)$, then $\operatorname{div} \mathbf{G} = 0$ and $\mathbf{G} \cdot \boldsymbol{n} = 0$ on $\partial\widetilde{\Omega}$, i.e., $\mathbf{G}$ belong to $\mathbf{H}_0(\operatorname{div}^0; \widetilde{\Omega}) := \{ \mathbf{u} \in \mathrm{L}^2(\widetilde{\Omega})^3 : \operatorname{div} \mathbf{u} = 0, \mathbf{u} \cdot \boldsymbol{n} = 0 \}$. Thus $\widehat{\mathrm{H}}_r^1(\Omega)$ can be identified with a closed subspace of $\mathbf{H}(\mathbf{curl}, \widetilde{\Omega}) \cap \mathbf{H}_0(\operatorname{div}^0; \widetilde{\Omega})$ continuously included in $\mathrm{H}^s(\widetilde{\Omega})^3$ for $s > 1/2$, which, in turn, is compactly included in $\mathrm{L}^2(\widetilde{\Omega})^3$ (see [14, Theorem I.1.3]). Then,

$$\widehat{\mathrm{H}}_r^1(\Omega) \subset \mathrm{L}_r^2(\Omega)$$

with compact inclusion and, hence, $\widetilde{\mathrm{H}}_r^1(\Omega)$ is also compactly included in $\mathrm{L}_r^2(\Omega)$.

6.2 Weak formulation

In order to give a weak formulation of the above problems, let us define the closed subspaces of $\widetilde{\mathrm{H}}_r^1(\Omega)$ and $\widehat{\mathrm{H}}_r^1(\Omega)$

$$\mathcal{U} := \left\{ G \in \widetilde{\mathrm{H}}_r^1(\Omega) : \; G|_\Gamma = 0 \right\},$$

$$\mathcal{W} := \left\{ G \in \widehat{\mathrm{H}}_r^1(\Omega) : \; rG|_\Gamma \; \text{is constant} \right\},$$

respectively. Hence, for each $t \in [0, T]$ a weak formulation of Problem 5.1 is given by:

Problem 6.1 *Given $g \in \mathrm{H}^2(0, T; \widetilde{\mathrm{H}}_r^{1/2}(\Gamma))$, $f \in \mathrm{H}^1(0, T; \mathcal{U}')$, $B_{D0} \in \mathrm{L}_r^2(\Omega)$, and $\xi : \Omega \to Y$, find $H_D \in \mathrm{L}^2(0, T; \widetilde{\mathrm{H}}_r^1(\Omega)) \cap \mathrm{L}^\infty(0, T; \mathrm{L}_r^2(\Omega))$ and $B_D \in \mathrm{L}^2(0, T; \mathrm{L}_r^2(\Omega))$ with $\partial_t B_D \in \mathrm{L}^2(0, T; \mathcal{U}')$, such that*

$$\left\langle \frac{\partial B_D}{\partial t}, G \right\rangle_{\mathcal{U},\mathcal{U}'} + \int_\Omega \frac{1}{\sigma r} \left(\frac{\partial(rH_D)}{\partial r} \frac{\partial(rG)}{\partial r} + \frac{\partial(rH_D)}{\partial z} \frac{\partial(rG)}{\partial z} \right) dr dz = \langle f, G \rangle_{\mathcal{U},\mathcal{U}'}$$

$$\forall G \in \mathcal{U}, \quad \text{a.e. in } [0, T],$$
$$B_D = \mu_0 \left(H_D + \mathcal{F}(H_D, \xi) \right) \quad \text{in } \Omega \times (0, T),$$
$$H_D = g \quad \text{on } \Gamma \times (0, T),$$
$$B_D|_{t=0} = B_{D0} \quad \text{in } \Omega.$$

We use the classical notation $\langle \cdot, \cdot \rangle_{\mathcal{U},\mathcal{U}'}$ for the duality product between $\mathcal{U}$ and its dual space $\mathcal{U}'$.

Before stating a weak formulation of Problem 5.2, we notice that if the boundary of Ω intersects the symmetry axis ($r = 0$), then $\psi(t)$ should be identically zero because r vanishes

there. In that case, (5.38) would become a homogeneous Dirichlet boundary condition and Problem 5.2 without condition (5.39) would be exactly Problem 5.1 with $g = 0$, so there is no reason for (5.39) to hold for a given $b(t)$. However, this does not happen in the application that motivates this problem in which the domain does not intersect the symmetry axis (see [28]). This is the reason why, from now on when dealing with Problem 5.2, we will assume that

$$\inf\{r > 0 : (r, z) \in \Omega\} > 0 \tag{6.41}$$

and, hence, $L_r^2(\Omega)$ and $L_{1/r}^2(\Omega)$ are both identical to $L^2(\Omega)$. Similarly, $\widehat{H}_r^1(\Omega)$ is identical to $H^1(\Omega)$.

Straightforward computations lead to the following weak formulation for Problem 5.2 (see [3]):

Problem 6.2 *Given* $b \in H^2(0, T)$, $f \in H^1(0, T; \mathcal{W}')$, $B_{N0} \in L_r^2(\Omega)$ *and* $\xi : \Omega \to Y$, *find* $H_N \in H^1(0, T; L_r^2(\Omega)) \cap L^\infty(0, T; \mathcal{W})$ *and* $B_N \in L^2(0, T; L_r^2(\Omega))$ *with* $\partial_t B_N \in L^2(0, T; \mathcal{W}')$, *such that*

$$\left\langle \frac{\partial B_N}{\partial t}, G \right\rangle_{\mathcal{W}, \mathcal{W}'} + \int_\Omega \frac{1}{\sigma r} \left(\frac{\partial(r H_N)}{\partial r} \frac{\partial(r G)}{\partial r} + \frac{\partial(r H_N)}{\partial z} \frac{\partial(r G)}{\partial r} \right) dr\, dz$$

$$= \langle f, G \rangle_{\mathcal{W}, \mathcal{W}'} + \left(b'(t) - \langle f, r^{-1} \rangle_{\mathcal{W}, \mathcal{W}'} \right) (rG)\,|_\Gamma \qquad \forall G \in \mathcal{W}, \quad \text{a.e. in } [0, T],$$

$$B_N = \mu_0 \left(H_N + \mathcal{F}(H_N, \xi) \right) \quad \text{in } \Omega \times (0, T),$$

$$B_N|_{t=0} = B_{N0} \quad \text{in } \Omega.$$

We introduce the following assumptions that will be used to prove the existence of a solution to Problem 6.1 and Problem 6.2:

H.1 $\mathcal{F} : L_r^2(\Omega; C([0, T]) \times Y) \to L_r^2(\Omega; C([0, T]))$ is causal, strongly continuous and piecewise monotone (cf. (3.4)–(3.6)). We also assume that $\mathcal{F}$ is *affinely bounded*, namely,

$$\exists L_{\mathcal{F}} > 0, \exists \tau \in L_r^2(\Omega) : \forall v \in L_r^2(\Omega; C([0, T])),$$
$$\|[\mathcal{F}(v, \xi)](r, z, \cdot)\|_{C([0,T])} \le L_{\mathcal{F}} \|v(r, z, \cdot)\|_{C([0,T])} + \tau(r, z) \quad \text{a.e. in } \Omega. \tag{6.42}$$

H.2 $\sigma : (0, T) \times \Omega \to \mathbb{R}$ belongs to $W^{1,\infty}(0, T; L^\infty(\Omega))$ and there exist non-negative constants σ_* and σ^* such that

$$\sigma_* \le \sigma(r, z, t) \le \sigma^* \quad \forall t \in [0, T], \text{ a.e. in } \Omega.$$

H.3 There exist $(H_{0D}, W_{0D}) \in \widetilde{H}_r^1(\Omega) \times L_r^2(\Omega)$ or $(H_{0N}, W_{0N}) \in \mathcal{W} \times L_r^2(\Omega)$, such that

$$B_{D0}(r, z) = \mu_0 \left(H_{0D} + W_{0D} \right)(r, z) \quad \text{and} \quad B_{N0}(r, z) = \mu_0 \left(H_{0N} + W_{0N} \right)(r, z) \quad \text{a.e in } \Omega.$$

Also, for each $t \in [0, T]$, let $a_t(\cdot, \cdot)$ be the bilinear form defined by

$$a_t(G_1, G_2) := \int_\Omega \frac{1}{\sigma(\cdot, t)} \left(\frac{1}{r} \frac{\partial(r G_1)}{\partial r} \frac{1}{r} \frac{\partial(r G_2)}{\partial r} + \frac{\partial G_1}{\partial z} \frac{\partial G_2}{\partial z} \right) r\, dr\, dz, \quad G_1, G_2 \in \widehat{H}_r^1(\Omega). \tag{6.43}$$

From assumption H.2 it is straightforward to obtain the following result (see [4, Lemma 2.1]):

Lemma 3 *The bilinear forms* $a_t : \widehat{H}_r^1(\Omega) \times \widehat{H}_r^1(\Omega) \to \mathbb{R}$, $t \in [0, T]$, *are continuous uniformly in* t *and they satisfy the Gårding's inequality*

$$a_t(G, G) + \lambda \|G\|_{L_r^2(\Omega)}^2 \ge \gamma \|G\|_{\widehat{H}_r^1(\Omega)}^2 \quad \forall G \in \widehat{H}_r^1(\Omega), \quad \forall t \in [0, T], \tag{6.44}$$

with $\lambda = \gamma = 1/\sigma^*$. *Moreover, there exists* $\gamma_u > 0$ *such that*

$$a_t(G, G) \ge \gamma_u \|G\|_{\widehat{H}_r^1(\Omega)}^2 \quad \forall G \in \mathcal{U}, \quad \forall t \in [0, T]. \tag{6.45}$$

27

Finally, we introduce the linear operator $A(t) : \widehat{H}_r^1(\Omega) \to \widehat{H}_r^1(\Omega)'$ induced by $a_t(\cdot, \cdot)$, namely,

$$\langle A(t)H, G\rangle_{\widehat{H}_r^1(\Omega), \widehat{H}_r^1(\Omega)'} := a_t(H, G) \quad \forall H, G \in \widehat{H}_r^1(\Omega).$$

Clearly $A(t)$ is linear and continuous, i.e., it belongs to $\mathcal{L}(\widehat{H}_r^1(\Omega), \widehat{H}_r^1(\Omega)')$, for all $t \in [0, T]$.

Remark 8 *From the definition of $a_t(\cdot, \cdot)$, it follows that $a_t : \widetilde{H}_r^1(\Omega) \times \widetilde{H}_r^1(\Omega) \to \mathbb{R}$, $t \in [0, T]$, are continuous uniformly in t, and therefore, the linear operator $A(t) : \widetilde{H}_r^1(\Omega) \to \widetilde{H}_r^1(\Omega)'$ belongs to $\mathcal{L}(\widetilde{H}_r^1(\Omega), \widetilde{H}_r^1(\Omega)')$ for all $t \in [0, T]$.*

The next section is devoted to study the existence of solution to Problems 6.1 and 6.2. The proof is carried out through three different steps: time discretization, a priori estimates and passage to the limit by using compactness. This approximation procedure is often used in the analysis of equations that include a memory operator since at any time-step we solve a stationary problem in which this operator is reduced to a standard nonlinear mapping.

6.3 Existence of solution

In this section we will prove that, under certain assumptions, there exist (H_N, B_N) solution of Problem 6.2.

6.3.1 Time discretization

Let us fix $m \in \mathbb{N}$ and set $\Delta t := T/m$. Now, for $n = 1, \ldots, m$, we define $t^n := n\Delta t$, $b^n := b(t^n)$, $\sigma^n(r, z) := \sigma(r, z, t^n)$, $f^n := f(t^n)$ and $A(t^n) := A^n$. Notation $\bar{\partial} z^n$ refers to the difference quotient

$$\bar{\partial} z^n := \frac{z^n - z^{n-1}}{\Delta t}.$$

A time discretization of Problem 6.2 based on backward Euler's scheme reads as follows:

Given $H_N^0 = H_{0N}$ and $W_N^0 = W_{0N}$ in Ω, find $H_N^n \in \mathcal{W}$ and $W_N^n \in L_r^2(\Omega)$, $n = 1, \ldots, m$, satisfying

$$\mu_0 \bar{\partial} H_N^n + \mu_0 \bar{\partial} W_N^n + A^n H_N^n = R_N^n \qquad \text{in } \mathcal{W}', \tag{6.46}$$

$$W_N^n = [\mathcal{F}(H_{N\Delta t^n}, \xi)](t^n), \tag{6.47}$$

where $H_{N\Delta t^n} : [0, t^n] \to \mathcal{W}$ is the piecewise linear in time interpolant of $\{H_N^i\}_{i=0}^n$ given by

$$H_{N\Delta t^n}(t^0) := H_{0N}; \tag{6.48}$$

$$H_{N\Delta t^n}(t) := H_N^{i-1} + (t - t^{i-1}) \bar{\partial} H_N^i, \quad t \in (t^{i-1}, t^i], \quad i = 1, \ldots, n, \tag{6.49}$$

and

$$\langle R_N^n, G\rangle_{\mathcal{W}, \mathcal{W}'} := \langle f^n, G\rangle_{\mathcal{W}, \mathcal{W}'} + \left(\bar{\partial} b^n - \langle f^n, r^{-1}\rangle_{\mathcal{W}, \mathcal{W}'}\right) (rG)|_\Gamma.$$

We notice that, since for $n \in \{1, \ldots, m\}$ we already know $H_N^1, \ldots, H_N^{n-1}$, we have that $W_N^n(\cdot) = [\mathcal{F}(H_{N\Delta t^n}, \xi)](\cdot, t^n)$ depends only on $H_{N\Delta t^n}(\cdot, t)|_{[0, t^{n-1}]}$, which is known, and on H_N^n, which must be determined.

In order to analyze the discrete problem, we define $F^n : \Omega \times \mathbb{R} \longrightarrow \mathbb{R}$ as follows: given $s \in \mathbb{R}$

$$F^n(r, z, s) := [\mathcal{F}(U_s, \xi)](r, z, t^n) \quad \text{a.e. in } \Omega,$$

with U_s the piecewise linear in time function such that $U_s(r, z, t^l) = H_N^l(r, z)$, $l = 0, \ldots, n-1$ and $U_s(r, z, t^n) = s$. This allows us to introduce the operator $\mathbb{F}^n : L_r^2(\Omega) \to L_r^2(\Omega)$ defined by $\mathbb{F}^n(G)(\cdot) := F^n(\cdot, G(\cdot))$ for all $G \in L_r^2(\Omega)$. The following lemma provides some properties of $\mathbb{F}^n$ that will be used in the sequel.

Lemma 4 *For all $n = 1, \ldots, m$, $\mathbb{F}^n : L_r^2(\Omega) \to L_r^2(\Omega)$ is a continuous and monotone operator. Moreover,*

$$\int_\Omega \mathbb{F}^n(G) G r \, dr dz \geq -C_1 \|G\|_{L_r^2(\Omega)} - C_2 \qquad \forall G \in L_r^2(\Omega), \tag{6.50}$$

where $C_1, C_2 > 0$ depend on $\{H_N^l\}_{l=0}^{n-1}$ but are independent of G.

Proof The continuity and non-decreasing properties of $\mathbb{F}^n$ follows from H.1 (cf. (3.5), (3.6) and (6.42)), whereas (6.50) is derived from (6.42). ∎

Thus, from the theory of monotone operators, it follows that (6.46)–(6.47) has a unique solution (see, for instance, [26, Theorem 2.18]).

6.3.2 A priori estimates

The aim of this section is to prove an a priori estimate for the solution of (6.46)–(6.47).

Here and thereafter C and c, with or without subscripts, will be used for positive constants not necessarily the same at each occurrence, but always independent of the time-step Δt.

Lemma 5 *There exists $C > 0$ such that, for all $l = 1, \ldots, m$,*

$$\Delta t \sum_{n=1}^l \|\bar\partial W_N^n\|_{\mathcal{W}'}^2 + \|H_N^l\|_{\widehat{H}_r^1(\Omega)}^2 + \Delta t \sum_{n=1}^l \|\bar\partial H_N^n\|_{L_r^2(\Omega)}^2 \leq C.$$

Proof Let apply (6.46) to $(H_N^n - H_N^{n-1})$. For $n = 1, \ldots, m$ we obtain

$$\mu_0 \Delta t \left\| \frac{H_N^n - H_N^{n-1}}{\Delta t} \right\|_{L_r^2(\Omega)}^2 + \int_\Omega \frac{\mu_0}{\Delta t}(W_N^n - W_N^{n-1})(H_N^n - H_N^{n-1}) + \langle A^n H_N^n, H_N^n - H_N^{n-1}\rangle_{\mathcal{W},\mathcal{W}'}$$

$$= \langle f^n, H_N^n - H_N^{n-1}\rangle_{\mathcal{W},\mathcal{W}'} + \left(\bar\partial b^n - \langle f^n, r^{-1}\rangle_{\mathcal{W},\mathcal{W}'}\right)\left(r H_N^n - r H_N^{n-1}\right)|_\Gamma. \tag{6.51}$$

First, we estimate the terms on the left hand side. From the piecewise monotonicity of $\mathcal{F}$ (cf. (3.6)) we have that

$$\int_\Omega \frac{1}{\Delta t}(W_N^n - W_N^{n-1})(H_N^n - H_N^{n-1}) \, dr dz \geq 0. \tag{6.52}$$

On the other hand, in order to estimate the last term on the left-hand side of (6.51) we use the identity $2(p-q)p = p^2 + (p-q)^2 - q^2$ to obtain that

$$2\langle A^n H_N^n, H_N^n - H_N^{n-1}\rangle_{\mathcal{W},\mathcal{W}'} \geq \langle A^n H_N^n, H_N^n\rangle_{\mathcal{W},\mathcal{W}'} - \langle A^n H_N^{n-1}, H_N^{n-1}\rangle_{\mathcal{W},\mathcal{W}'}$$

$$= \langle A^n H_N^n, H_N^n\rangle_{\mathcal{W},\mathcal{W}'} - \langle A^{n-1} H_N^{n-1}, H_N^{n-1}\rangle_{\mathcal{W},\mathcal{W}'} + \langle (A^{n-1} - A^n) H_N^{n-1}, H_N^{n-1}\rangle_{\mathcal{W},\mathcal{W}'} \tag{6.53}$$

where

$$\left|\langle (A^{n-1} - A^n) H_N^{n-1}, H_N^{n-1}\rangle_{\mathcal{W},\mathcal{W}'}\right| \leq C_\sigma \|\partial_t \sigma\|_{L^\infty(0,T;L^\infty(\Omega))} \Delta t \|H_N^{n-1}\|_{\widehat{H}_r^1(\Omega)}^2. \tag{6.54}$$

Summing up (6.51) for $n = 1, \ldots, l$ with $l \in \{1, \ldots, m\}$, from (6.52)–(6.54) we obtain

$$\sum_{n=1}^{l} \mu_0 \Delta t \left\| \bar{\partial} H_N^n \right\|_{\mathrm{L}_r^2(\Omega)}^2 + \frac{1}{2} \langle A^l H_N^l, H_N^l \rangle_{\mathcal{W}, \mathcal{W}'}$$

$$\leq \frac{1}{2} \langle A^0 H_{0N}, H_{0N} \rangle_{\mathcal{W}, \mathcal{W}'} + \sum_{n=1}^{l} C_\sigma \left\| \partial_t \sigma \right\|_{\mathrm{L}^\infty(0,T;\mathrm{L}^\infty(\Omega))} \Delta t \left\| H_N^{n-1} \right\|_{\widehat{\mathrm{H}}_r^1(\Omega)}^2$$

$$+ \sum_{n=1}^{l} \langle f^n, H_N^n - H_N^{n-1} \rangle_{\mathcal{W}, \mathcal{W}'} + \sum_{n=1}^{l} \left(\bar{\partial} b^n - \langle f^n, r^{-1} \rangle_{\mathcal{W}, \mathcal{W}'} \right) \left(r H_N^n - r H_N^{n-1} \right) |_\Gamma. \tag{6.55}$$

Next, we estimate the last two terms on the right-hand side of (6.55). By summation by parts, Young's inequality and the fact that $(rG)|_\Gamma \leq C \|G\|_{\widehat{\mathrm{H}}_r^1(\Omega)} \ \forall G \in \mathcal{W}$, we have that

$$\left| \sum_{n=1}^{l} \left(\bar{\partial} b^n - \langle f^n, r^{-1} \rangle_{\mathcal{W}, \mathcal{W}'} \right) \left(r H_N^n - r H_N^{n-1} \right) |_\Gamma \right|$$

$$= \left| \left(\bar{\partial} b^l - \langle f^l, r^{-1} \rangle_{\mathcal{W}, \mathcal{W}'} \right) \left(r H_N^l \right) |_\Gamma - \left(\bar{\partial} b^1 - \langle f^1, r^{-1} \rangle \right) \left(r H_{0N} \right) |_\Gamma \right.$$

$$\left. - \sum_{n=1}^{l-1} \left(\bar{\partial} b^{n+1} - \bar{\partial} b^n - \langle f^{n+1} - f^n, r^{-1} \rangle_{\mathcal{W}, \mathcal{W}'} \right) \left(r H_N^n \right) |_\Gamma \right|$$

$$\leq C_\varepsilon \left\{ \|b\|_{\mathrm{H}^2(0,T)}^2 + \|f\|_{\mathrm{H}^1(0,T;\mathcal{W}')}^2 + \Delta t \sum_{n=1}^{l-1} \left| \frac{\bar{\partial} b^{n+1} - \bar{\partial} b^n}{\Delta t} \right|^2 + \Delta t \sum_{n=1}^{l-1} \left\| \bar{\partial} f^{n+1} \right\|_{\mathcal{W}'}^2 \right\}$$

$$+ \varepsilon \left\| H_N^l \right\|_{\widehat{\mathrm{H}}_r^1(\Omega)}^2 + \Delta t \sum_{n=1}^{l-1} \|H_N^n\|_{\widehat{\mathrm{H}}_r^1(\Omega)}^2 + \|H_{0N}\|_{\widehat{\mathrm{H}}_r^1(\Omega)}^2. \tag{6.56}$$

In a similar way,

$$\left| \sum_{n=1}^{l} \langle f^n, H_N^n - H_N^{n-1} \rangle_{\mathcal{W}, \mathcal{W}'} \right| \leq C_\varepsilon \|f\|_{\mathrm{H}^1(0,T;\mathcal{W}')}^2 + \varepsilon \left\| H_N^l \right\|_{\widehat{\mathrm{H}}_r^1(\Omega)}^2$$

$$+ \Delta t \sum_{n=1}^{l-1} \|H_N^n\|_{\widehat{\mathrm{H}}_r^1(\Omega)}^2 + \|H_{0N}\|_{\widehat{\mathrm{H}}_r^1(\Omega)}^2, \tag{6.57}$$

for all $\varepsilon > 0$. On the other hand, in order to deal with the second term on the left-hand side of (6.55), we first notice that $H_N^l = H_{0N} + \Delta t \sum_{n=1}^{l} \bar{\partial} H_N^n$ and then

$$\Delta t \sum_{n=1}^{l} \left\| \bar{\partial} H_N^n \right\|_{\mathrm{L}_r^2(\Omega)}^2 \geq \frac{1}{T} \left\{ \frac{\left\| H_N^l \right\|_{\mathrm{L}_r^2(\Omega)}^2}{2} - \|H_{0N}\|_{\mathrm{L}_r^2(\Omega)}^2 \right\}.$$

Hence, from Lemma 3 (cf. (6.44)) we obtain that there exists $\widehat{\gamma} := \min\left\{ \frac{\mu_0}{4T}, \frac{1}{2} \right\} \gamma$, such that

$$\mu_0 \Delta t \sum_{n=1}^{l} \left\| \bar{\partial} H_N^n \right\|_{\mathrm{L}_r^2(\Omega)}^2 + \frac{1}{2} \langle A^l H_N^l, H_N^l \rangle_{\mathcal{W}, \mathcal{W}'}$$

$$\geq \frac{\Delta t \mu_0}{2} \sum_{n=1}^{l} \left\| \bar{\partial} H_N^i \right\|_{\mathrm{L}_r^2(\Omega)}^2 + \widehat{\gamma} \left\| H_N^l \right\|_{\widehat{\mathrm{H}}_r^1(\Omega)}^2 - \mu_0 \frac{\|H_{0N}\|_{\mathrm{L}_r^2(\Omega)}^2}{2T}. \tag{6.58}$$

Then, by replacing (6.56)–(6.58) into (6.55) and choosing $\varepsilon = \dfrac{\widehat{\gamma}}{4}$ we obtain

$$\frac{\mu_0 \Delta t}{2} \sum_{n=1}^{l} \left\| \bar{\partial} H_N^n \right\|_{\mathrm{L}_r^2(\Omega)}^2 + \frac{\widehat{\gamma}}{2} \left\| H_{\Delta t}^l \right\|_{\widehat{\mathrm{H}}_r^1(\Omega)}^2$$

$$\leq C \left\{ \|b\|_{\mathrm{H}^2(0,T)}^2 + \|f\|_{\mathrm{H}^1(0,T;\mathcal{W}')}^2 + \Delta t \sum_{n=1}^{l} \left| \frac{\bar{\partial} b^n - \bar{\partial} b^{n-1}}{\Delta t} \right|^2 + \Delta t \sum_{n=1}^{l} \left\| \bar{\partial} f^n \right\|_{\mathcal{W}'}^2 \right\}$$

$$+ C \Delta t \sum_{n=1}^{l} \left\| H_N^{n-1} \right\|_{\widehat{\mathrm{H}}_r^1(\Omega)}^2 + \left(\frac{\mu_0}{2T} + \frac{1}{2\sigma_*} + 2 \right) \|H_{0N}\|_{\widehat{\mathrm{H}}_r^1(\Omega)}^2 .$$

Hence, by using the discrete Gronwall's lemma we obtain

$$\Delta t \sum_{n=1}^{l} \left\| \bar{\partial} H_N^n \right\|_{\mathrm{L}_r^2(\Omega)}^2 + \left\| H_{\Delta t}^l \right\|_{\widehat{\mathrm{H}}_r^1(\Omega)}^2 \leq C, \qquad l = 1, \dots, m,$$

with $C > 0$ depending on $\|b\|_{\mathrm{H}^2(0,T)}$, $\|H_{0N}\|_{\widehat{\mathrm{H}}_r^1(\Omega)}$, $\|f\|_{\mathrm{H}^1(0,T;\mathcal{W}')}$ and $\|\sigma\|_{\mathrm{W}^{1,\infty}(0,T;\mathrm{L}^\infty(\Omega))}$. Finally, we estimate $\sum_{n=1}^{l} \left\| \bar{\partial} W_N^n \right\|_{\mathcal{W}'}^2$ by using (6.46) and the last inequality. ∎

6.3.3 Convergence

Now, we will define a family of approximate solutions to Problem 6.2 and prove its weak convergence to a solution. With this aim, we introduce some notation: let $W_{N\Delta t} : [0, T] \to \mathrm{L}_r^2(\Omega)$ be the piecewise linear in time interpolant of $\{W_N^n\}_{n=0}^m$ (cf. (6.48)–(6.49)). We also introduce the step function $\overline{H}_{N\Delta t} : [0, T] \to \mathcal{W}$ by:

$$\overline{H}_{N\Delta t}(t^0) := H_{0N}; \quad \overline{H}_{N\Delta t}(t) := H_N^n, \quad t \in (t^{n-1}, t^n], \quad i = n, \dots, m, \qquad (6.59)$$

and define the step functions $\overline{A}_{\Delta t}$ and $\overline{R}_{N\Delta t}$ in a similar way.

Using the above notation we rewrite equation (6.46) as follows:

$$\mu_0 \frac{\partial H_{N\Delta t}}{\partial t} + \mu_0 \frac{\partial W_{N\Delta t}}{\partial t} + \overline{A}_{\Delta t} \overline{H}_{N\Delta t} = \overline{R}_{N\Delta t} \quad \text{in } \mathcal{W}', \quad \text{a.e. in } (0, T). \qquad (6.60)$$

From Lemma 5 we deduce that there exists $C > 0$ such that

$$\left\| \frac{\partial W_{N\Delta t}}{\partial t} \right\|_{\mathrm{L}^2(0,T;\mathcal{W}')} + \left\| \overline{A}_{\Delta t} \overline{H}_{N\Delta t} \right\|_{\mathrm{L}^\infty(0,T;\mathcal{W}')}$$

$$+ \|H_{N\Delta t}\|_{\mathrm{H}^1(0,T;\mathrm{L}_r^2(\Omega)) \cap \mathrm{L}^\infty(0,T;\widehat{\mathrm{H}}_r^1(\Omega))} + \left\| \overline{H}_{N\Delta t} \right\|_{\mathrm{L}^\infty(0,T;\widehat{\mathrm{H}}_r^1(\Omega))} \leq C. \qquad (6.61)$$

Moreover, since $\mathrm{H}^1(0, T; \mathrm{L}_r^2(\Omega)) = \mathrm{L}_r^2(\Omega; \mathrm{H}^1(0, T)) \hookrightarrow \mathrm{L}_r^2(\Omega; C([0, T]))$ with continuous injection, by using the affinely bounded assumption and (6.61) it follows that there exist $L_{\mathcal{F}} > 0$ and $\tau \in \mathrm{L}_r^2(\Omega)$ such that

$$\|W_{N\Delta t}\|_{\mathrm{L}_r^2(\Omega \times [0,T])} \leq \sqrt{T} \|W_{N\Delta t}\|_{\mathrm{L}_r^2(\Omega; C([0,T]))} \leq \sqrt{T} L_{\mathcal{F}} \|H_{N\Delta t}\|_{\mathrm{L}_r^2(\Omega; C([0,T]))} + \sqrt{T} \|\tau\|_{\mathrm{L}_r^2(\Omega)} \leq C.$$

This allows us to conclude that there exists H_N, W_N and X such that,

$$H_{N\Delta t} \longrightarrow H_N \quad \text{in } \mathrm{H}^1(0, T; \mathrm{L}_r^2(\Omega)) \cap \mathrm{L}^\infty(0, T; \widehat{\mathrm{H}}_r^1(\Omega)) \text{ weakly star}, \qquad (6.62)$$

$$\overline{H}_{N\Delta t} \longrightarrow H_N \quad \text{in } \mathrm{L}^\infty(0, T; \widehat{\mathrm{H}}_r^1(\Omega)) \text{ weakly star}, \qquad (6.63)$$

$$W_{N\Delta t} \longrightarrow W_N \quad \text{in } \mathrm{L}_r^2(\Omega \times [0, T]) \text{ weakly}, \qquad (6.64)$$

$$\frac{\partial}{\partial t} H_{N\Delta t} \longrightarrow \frac{\partial}{\partial t} H_N \quad \text{in } \mathrm{L}^2(0, T; \mathcal{W}') \text{ weakly}, \qquad (6.65)$$

$$\frac{\partial}{\partial t} W_{N\Delta t} \longrightarrow \frac{\partial}{\partial t} W_N \quad \text{in } \mathrm{L}^2(0, T; \mathcal{W}') \text{ weakly}, \qquad (6.66)$$

$$\overline{A}_{\Delta t} \overline{H}_{N\Delta t} \longrightarrow X \quad \text{in } \mathrm{L}^\infty(0, T; \mathcal{W}') \text{ weakly star}. \qquad (6.67)$$

31

Let $R_N \in \mathrm{H}^1(0, T; \mathcal{W}')$ defined by

$$\langle R_N, G \rangle_{\mathcal{W}, \mathcal{W}'} := \langle f, G \rangle_{\mathcal{W}, \mathcal{W}'} + \left(b'(t) - \langle f, r^{-1} \rangle_{\mathcal{W}, \mathcal{W}'} \right) (rG)|_\Gamma \qquad \forall G \in \mathcal{W}, \quad \text{a.e. in } [0, T].$$

By passing to the limit in (6.60) we obtain

$$\mu_0 \frac{\partial H_N}{\partial t} + \mu_0 \frac{\partial W_N}{\partial t} + X = R_N \qquad \text{in } \mathcal{W}', \quad \text{a.e. in } (0, T), \tag{6.68}$$

because $\overline{R}_{N\Delta t} \to R_N$ in $\mathrm{L}^2(0, T; \mathcal{W}')$, for $f \in \mathrm{H}^1(0, T; \mathcal{W}')$ and $b \in \mathrm{H}^2(0, T)$. The next step is to prove that $X = AH_N$ and $W_N = \mathcal{F}(H_N, \xi)$. The first equality, follows from (6.63), (6.67) and H.2. To prove the latter, first we recall that by virtue of the assumption on the domain (6.41), $\mathrm{L}_r^2(\Omega)$ and $\widehat{\mathrm{H}}_r^1(\Omega)$ are both identical to $\mathrm{L}^2(\Omega)$ and $\mathrm{H}^1(\Omega)$, respectively. Therefore, the last equality follows from the inclusions

$$\mathrm{H}^1(0, T; \mathrm{L}_r^2(\Omega)) \cap \mathrm{L}^2(0, T; \widehat{\mathrm{H}}_r^1(\Omega)) \subset \mathrm{H}^s(\Omega; \mathrm{H}^{1-s}(0, T)) \subset \mathrm{L}_r^2(\Omega; C([0, T])) \qquad s \in (0, 1/2), \tag{6.69}$$

being the first continuous and the latter compact (see [34, Chapter IX, (1.45)]), and the strong continuity of $\mathcal{F}$.

As a consequence of this, we obtain the following result.

Theorem 6.1 *Let us assume hypotheses H.1, H.2 and H.3. Then, Problem 6.2 has a solution.*

Proof From (6.68) it follows that

$$\left\langle \frac{\partial B_N}{\partial t}, G \right\rangle_{\mathcal{W}, \mathcal{W}'} + a_t(H_N, G)$$
$$= \langle f, G \rangle_{\mathcal{W}, \mathcal{W}'} + \left(b'(t) - \langle f, r^{-1} \rangle_{\mathcal{W}, \mathcal{W}'} \right) (rG)|_\Gamma \qquad \forall G \in \mathcal{W}, \quad \text{a.e. in } [0, T],$$
$$B_N = \mu_0 \left(H_N + \mathcal{F}(H_N, \xi) \right) \quad \text{in } \Omega \times (0, T).$$

Moreover, from the compact inclusion (6.69) and the strongly continuous assumption (cf. (3.5)) we have that $H_{N\Delta t}(0) \to H_N(0)$ and $W_{N\Delta t}(0) \to \mathcal{F}(H_N, \xi)(0)$ in $\mathrm{L}_r^2(\Omega)$. Therefore (H_N, B_N) is a solution to Problem 6.2. $\blacksquare$

A similar result hold for Problem 6.1.

Theorem 6.2 *Let us assume hypotheses H.1, H.2 and H.3. Then Problem 6.1 has a solution.*

Proof We only give a sketch of the proof. First, we consider a lifting of the boundary data. We notice that, from the regularity of g, there exists $H_g \in \mathrm{H}^2(0, T; \widetilde{\mathrm{H}}_r^1(\Omega))$ such that $H_g|_\Gamma = g$ and

$$\|H_g\|_{\mathrm{H}^k(0, T; \widetilde{\mathrm{H}}_r^1(\Omega))} \leq C \|g\|_{\mathrm{H}^k(0, T; \widetilde{\mathrm{H}}_r^{1/2}(\Gamma))}, \qquad k = 1, 2, \tag{6.70}$$

being C a constant independent of g (cf. [4, Section 2.3]). Then, we write $H_D = H_u + H_g$ with $H_u \in \mathcal{U}$, so that the existence of weak solutions can be deduced by applying arguments similar to those used to prove the existence of solution to Problem 6.2 (see also [34, Chapter IX]). Although the latter does not consider weighted Sobolev spaces, minor modifications of their arguments lead to the existence of solution to Problem 6.1. In particular, we obtain the corresponding compactness result (cf. (6.69)) by identifying the axisymmetric space $\mathrm{H}^1(0, T; \mathrm{L}_r^2(\Omega)) \cap \mathrm{L}^\infty(0, T; \widetilde{\mathrm{H}}_r^1(\Omega))$ with its respective 3D version $\mathrm{H}^1(0, T; \mathrm{L}^2(\widetilde{\Omega})^3) \cap \mathrm{L}^\infty(0, T; \mathrm{H}^1(\widetilde{\Omega})^3) \subset \mathbf{L}^2(\widetilde{\Omega}; C([0, T]))$, the latter with compact inclusion.

Remark 9 *There is not a uniqueness result for a generic hysteresis operator satisfying (3.4)–(3.6), even though it is possible to prove such a result by choosing a particular operator, for instance, the Prandtl-Ishlinskii operator of play type (see, for instance, [16] and more recently [11, Theorem 5.1]).*

To end this section, notice that, from Lemma 2 we obtain the following existence result.

Theorem 6.3 *Let us assume that H.2 and H.3 hold true. Then, by choosing as hysteresis operator in the constitutive equations (5.33) and (5.37) the classical Preisach operator $\mathcal{F}$ (cf. (4.7) and (4.8)), it follows that there exist (H_D, B_D) and (H_N, B_N) solutions to Problems 6.1 and 6.2, respectively.*

7 Numerical approximation

In this section we present a numerical implementation to solve a full discretization of Problem 6.1. The same procedure can be straightforwardly extended to solve Problem 6.2. For the sake of simplicity, in what follows we will drop subscript D. Let us recall that different algorithms have been proposed to approximate non-linear partial differential equation with hysteresis; see, for instance [30, 31, 28, 29].

From now on we will assume that Ω is a convex polygon. We associate a family of partitions $\{\mathcal{T}_h\}_{h>0}$ of Ω into triangles, where h denotes the mesh size. Let $\mathcal{V}_h$ be the space of continuous piecewise linear finite elements vanishing on the symmetry axis $(r = 0)$, so that $\mathcal{V}_h \subset \widetilde{H}^1_r(\Omega)$. We also consider the finite-dimensional space $\mathcal{U}_h := \mathcal{V}_h \cap \mathcal{U}$ and denote by $\mathcal{V}_h(\Gamma)$ the space of traces on Γ of functions in $\mathcal{V}_h$.

By using the above finite element space for the space discretization and the backward Euler scheme for time discretization, we are led to the following Galerkin approximation of Problem 6.1:

Problem 7.1 *Given $B_h^0 = \mu_0 \left(H_h^0 + W_0 \right)$ with $H_h^0 \in \mathcal{V}_h$ and $W_0 \in L^2_r(\Omega)$, find $H_h^n \in \mathcal{V}_h$ and $B_h^n \in L^2_r(\Omega)$, $n = 1, \ldots, m$, such that*

$$\frac{1}{\Delta t} \int_\Omega B_h^n G_h r \, drdz + \int_\Omega \frac{1}{\sigma^n r} \left(\frac{\partial (rH_h^n)}{\partial r} \frac{\partial (rG_h)}{\partial r} + \frac{\partial (rH_h^n)}{\partial z} \frac{\partial (rG_h)}{\partial z} \right) drdz$$

$$= \langle f^n, G_h \rangle_{\mathcal{U}, \mathcal{U}'} + \frac{1}{\Delta t} \int_\Omega B_h^{n-1} G_h r \, drdz \qquad \forall G_h \in \mathcal{U}_h,$$

$$B_h^n(r, z) = \mathcal{B}^n(H_h^n)(r, z) \quad a.e. \ in \ \Omega,$$

$$H_h^n = g_h^n \quad on \ \Gamma,$$

where $H_h^0 \in \mathcal{V}_h$ and $g_h^n \in \mathcal{V}_h(\Gamma)$ are convenient approximations of $H_0 \in \widetilde{H}^1_r(\Omega)$ (cf. H.3) and $g(t^n)$, for $n = 1, \ldots, m$, respectively, and $\mathcal{B}^n : L^2_r(\Omega) \to L^2_r(\Omega)$, $n = 1, \ldots, m$, is such that, given $u \in L^2_r(\Omega)$, and an initial state ξ

$$\mathcal{B}^n(u)(r, z) := \mu_0 \left(u(r, z) + [\mathcal{F}(U_{h\Delta t^n}, \xi)](r, z, t^n) \right) \quad \text{a.e. in } \Omega, \tag{7.71}$$

with $U_{h\Delta t^n}$ being the piecewise linear in time function such that $U_{h\Delta t^n}(r, z, t^l) = H_h^l(r, z)$, $l = 0, \ldots, n-1$, and $U_{h\Delta t^n}(r, z, t^n) = u(r, z)$ a.e. in Ω.

At each time step of the above algorithm, we must solve a non-linear problem. With this purpose, we have used a duality iterative algorithm which is based on some properties of the Yosida regularization of maximal monotone operators. This algorithm, introduced by
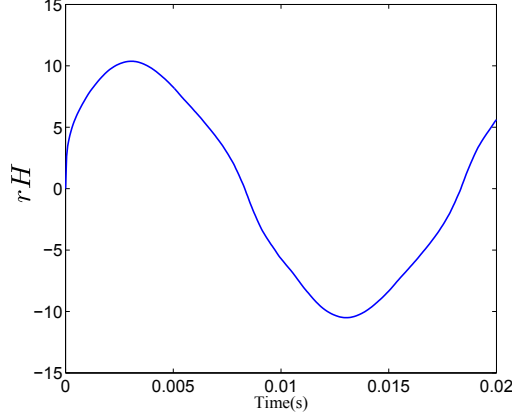
Figure 27: rH on the boundary.

Bermúdez and Moreno [5], has been extensively used for a wide range of applications with good numerical results. It seems to be very promising to handle the hysteresis non-linearity because it takes advantage of the spatial independence of the hysteresis operator.

In order to complete the proposed numerical scheme, a particular hysteresis operator must be considered (cf. (7.71)). In view of applications we have considered the classical Preisach model described in Section 4.

8   Numerical example

In this section we report the results of a numerical test obtained with a Fortran code implementing the numerical method described in Section 7 to approximate the solution to Problem 6.1.

Let us consider the eddy current Problem 6.1 with $\Omega := [R_1, R_2] \times [0, d]$ and the non-homogeneous Dirichlet condition given by $g = (rH)/(2\pi r)$ where the constant value $rH(t)$ on the boundary is depicted in Figure 27 as a function of time which has been taken from a numerical simulation with the code described in [3]. The geometrical and physical data have been summarized in Table 1 below.

Table 1: Geometrical and physical data for the test

Internal radius, R_1:	0.0825 m
External radius, R_2:	0.0925 m
Thickness, d:	0.00065 m
Electrical conductivity, σ:	4×10^6 (Ohm/m)$^{-1}$
Frequency, f:	50 Hz

In practical applications the measurable data is the B-H curve, usually represented by the Everett function. We assume that the B-H relation (cf. (5.33)) is given by the Preisach operator characterized by the Everett function depicted in Figure 28 (left) which comes from experimental measurements. Figure 28 (right) shows the major loop of the B-H curve obtained with this Everett function.
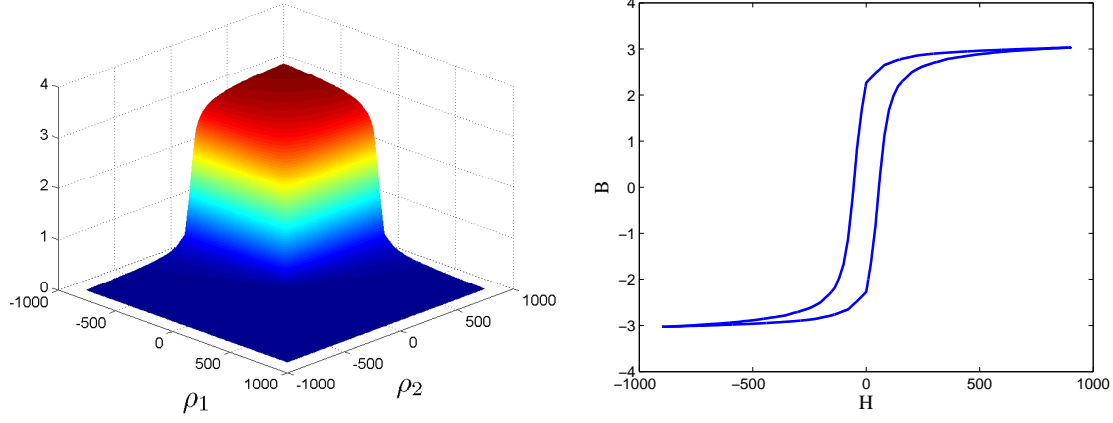
Figure 28: Everett function (left) and the corresponding B-H curve (right).

Figure 29 (left) shows the evolution of the B-H curve in a fixed point of the mesh and Figure 29 (right) the waveforms in the middle and at the surface of the domain. Whereas Figure 30 shows the magnetic field and magnetic induction, at different times on a fixed domain. In Figure 29 (right), we can see the presence of skin effect.
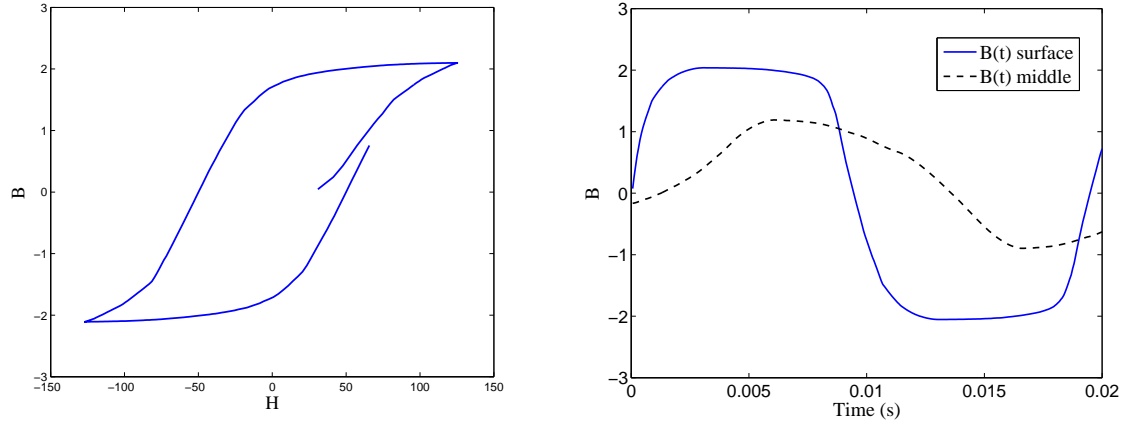

Figure 29: B-H curve at the surface of the domain (left) and B vs. time in the middle and at the surface of the domain (right).
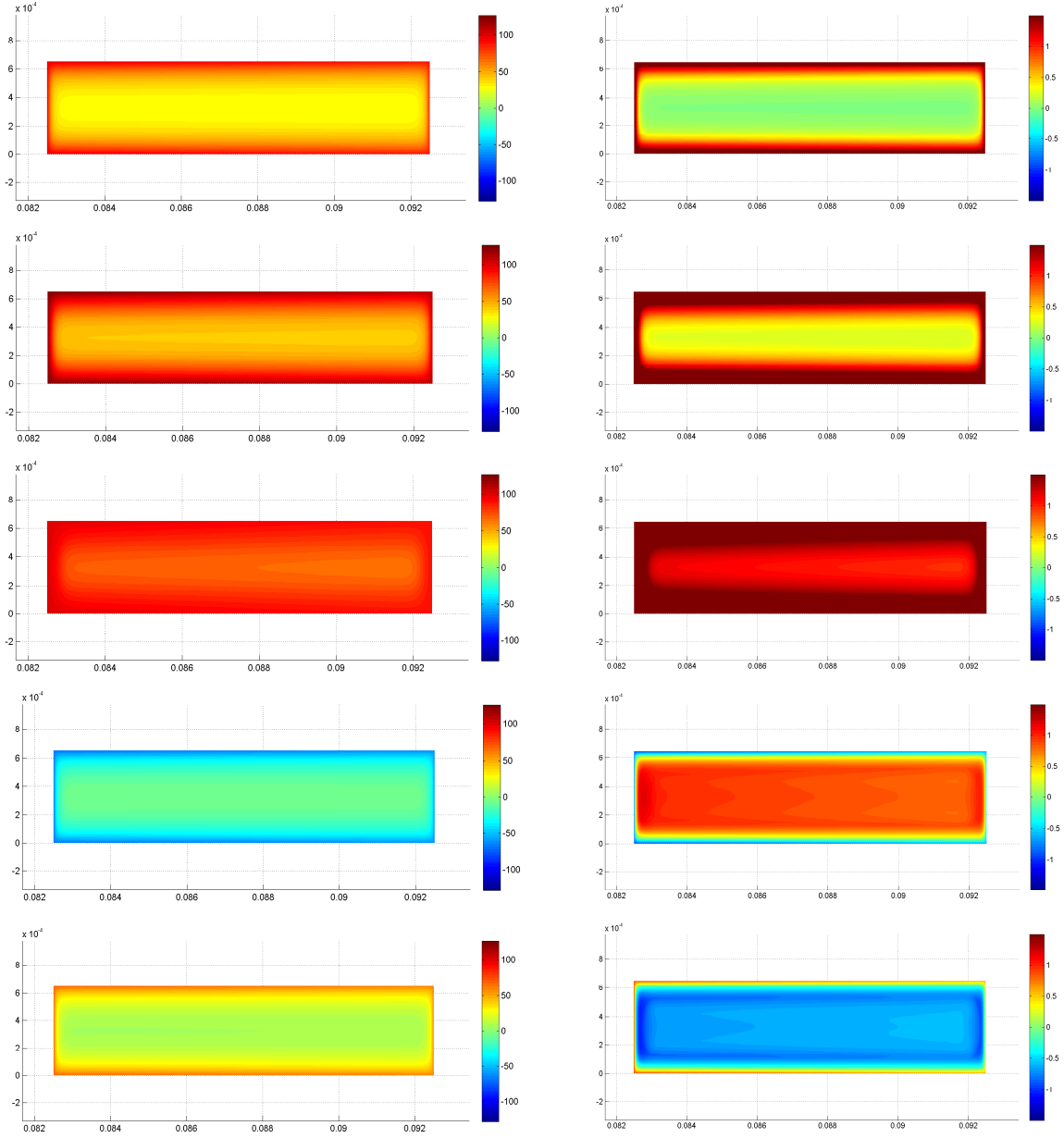
Figure 30: Magnetic field H (left) and magnetic induction B (right) at times $t = 0.00125$, 0.0025, 0.0050, 0.0100 and 0.0200 s.

References

[1] A. Bermúdez, J. Bullón, and F. Pena, *A finite element method for the thermoelectrical modelling of electrodes*, Commun. Numer. Meth. Eng. **14** (1998), 581–593.

[2] A. Bermúdez, J. Bullón, F. Pena, and P. Salgado, *A numerical method for transient simulation of metallurgical compound electrodes*, Finite Elem. Anal. Des. **39** (2003), 283–299.

[3] A. Bermúdez, D. Gómez, R. Rodríguez, P. Salgado, and P. Venegas, *Numerical solution of a transient non-linear axisymmetric eddy current model with non-local boundary conditions*, Math. Models Methods Appl. Sci. **23** (2013), 2495–2521.

[4] A. Bermúdez, D. Gómez, R. Rodríguez, and P. Venegas, *Numerical analysis of a transient non-linear axisymmetric eddy current model*, (2013), (Submitted).

[5] A. Bermúdez and C. Moreno, *Duality methods for solving variational inequalities*, Comput. Math. Appl. **7** (1981), 43–58.

[6] G. Bertotti, *Hysteresis in Magnetism*, Academic Press, 1998.

[7] G. Bertotti and I. D. Mayergoyz (eds.), *The Science of Hysteresis. Vol. I*, Elsevier/Academic Press, Amsterdam, 2006.

[8] M. Brokate and J. Sprekels, *Hysteresis and Phase Transitions*, Springer, Berlin, 1996.

[9] L.R. Egan and E.P. Furlani, *A computer simulation of an induction heating system*, IEEE Trans. Magn. **27** (1991), 4343 – 4354.

[10] M. Eleuteri, *An existence result for a P.D.E. with hysteresis, convection and a nonlinear boundary condition*, Discrete Contin. Dyn. Syst. (2007), 344–353.

[11] ———, *Wellposedness results for a class of parabolic partial differential equations with hysteresis*, NoDEA Nonlinear Differential Equations Appl. **15** (2008), 557–580.

[12] M. Eleuteri and P. Krejčí, *Asymptotic behavior of a Neumann parabolic problem with hysteresis*, ZAMM Z. Angew. Math. Mech. **87** (2007), 261–277.

[13] ———, *An asymptotic convergence result for a system of partial differential equations with hysteresis*, Commun. Pure Appl. Anal. **6** (2007), 1131–1143.

[14] V. Girault and P.-A Raviart, *Finite Element Approximations of the Navier-Stokes Equations, Theory and Algorithms*, Springer, Berlin, 1986.

[15] J. Gopalakrishnan and J. E. Pasciak, *The convergence of V-cycle multigrid algorithms for axisymmetric Laplace and Maxwell equations*, Math. Comp. **75** (2006), 1697–1719.

[16] M. Hilpert, *On uniqueness for evolution problems with hysteresis*, Mathematical models for phase change problems, Internat. Ser. Numer. Math., vol. 88, Birkhäuser, Basel, 1989, pp. 377–388.

[17] R. Innvær and L. Olsen, *Practical use of mathematical models for Søderberg electrodes*, Elkem Carbon Technical Paper presented at the A.I.M.E. Conference (1980).

[18] M.A. Krasnosel'skiĭ and A.V. Pokrovskiĭ, *System with Hysteresis*, Springer, Berlin, 1989, (Russian edition, Nauka, Moscow (1983)).

[19] M. Markovic and Y. Perriard, *Eddy current power losses in a toroidal laminated core with rectangular cross section*, 2009 International Conference on Electrical Machines and Systems (ICEMS) (New York), IEEE, 2009, pp. 1249–1252.

[20] I.D. Mayergoyz, *Mathematical Models of Hysteresis*, Springer, New York, 1991.

[21] I.D. Mayergoyz and G. Friedman, *Isotropic vector Preisach model of hysteresis*, J. Appl. Phys. **61** (1987), 4022–4024.

[22] K.V. Namjoshi, J.D. Lavers, and P.P. Biringer, *Eddy-current power loss in toroidal cores with rectangular cross section*, IEEE Trans. Magn. **34** (1998), 636 –641.

[23] K. Preis, *A contribution to eddy current calculations in plane and axisymmetric multi-conductor systems*, IEEE Trans. Magn. **19** (1983), 2397–2400.

[24] F. Preisach, *Über die magnetische nachwirkung*, Zeitschrift für Physik, **94** (1935), 277–302.

[25] E. Rothe, *Zweidimensionale parabolische Randwertaufgaben als Grenzfall eindimensionaler Randwertaufgaben*, Math. Ann. **102** (1930), 650–670.

[26] T. Roubíček, *Non Linear Partial Differential Equations with Applications*, Birkhäuser, 2005.

[27] R. E. Showalter, Little T. D., and U. Hornung, *Parabolic pde with hysteresis*, 1996.

[28] R. Van Keer, L. Dupré, and J. A. A. Melkebeek, *On a numerical method for 2D magnetic field computations in a lamination with enforced total flux*, J. Comput. Appl. Math. **72** (1996), 179–191.

[29] _____, *Computational methods for the evaluation of the electromagnetic losses in electrical machinery*, Arch. Comput. Methods Engrg. **5** (1998), 385–443.

[30] C. Verdi and A. Visintin, *Numerical approximation of hysteresis problems*, IMA J. Numer. Anal. **5** (1985), 447–463.

[31] _____, *Numerical approximation of the Preisach model for hysteresis*, RAIRO Modél. Math. Anal. Numér. **23** (1989), 335–356.

[32] A. Visintin, *A model for hysteresis of distributed systems*, Ann. Mat. Pura Appl. **131** (1982), 203–231.

[33] _____, *On the Preisach model for hysteresis*, Nonlinear Anal. T.M.A. **8** (1984), 977–996.

[34] _____, *Differential models of hysteresis*, Springer, Berlin, 1994.

Centro de Investigación en Ingeniería Matemática (CI²MA)

PRE-PUBLICACIONES 2013 - 2014

2013-16 FABIÁN FLORES-BAZÁN: *A Fritz John necessary optimality condition of the alternative-type*

2013-17 VERONICA ANAYA, DAVID MORA, RICARDO RUIZ-BAIER: *An augmented mixed finite element method for the vorticity-velocity-pressure formulation of the Stokes equations*

2013-18 FERNANDO BETANCOURT, RAIMUND BÜRGER, STEFAN DIEHL, SEBASTIAN FARÅS: *A model of clarifier-thickener control with time-dependent feed properties*

2013-19 GABRIEL N. GATICA, ANTONIO MARQUEZ, RICARDO OYARZÚA, RAMIRO REBOLLEDO: *Analysis of an augmented fully-mixed approach for the coupling of quasi-Newtonian fluids and porous media*

2013-20 SERGIO CAUCAO, DAVID MORA, RICARDO OYARZÚA: *Analysis of a mixed-FEM for the pseudostress-velocity formulation of the Stokes problem with varying density*

2013-21 ERWAN HINGANT, MAURICIO SEPÚLVEDA: *On a sorption-coagulation equation: statement, existence and numerical approximation*

2013-22 VERONICA ANAYA, MOSTAFA BENDAHMANE, MICHAEL LANGLAIS, MAURICIO SEPÚLVEDA: *A convergent finite volume method for a model of indirectly transmitted diseases with nonlocal cross-diffusion*

2013-23 TOMÁS BARRIOS, ROMMEL BUSTINZA, VÍCTOR DOMÍNGUEZ: *On the discontinuous Galerkin method for solving boundary problems for the Helmholtz equation: A priori and a posteriori error analyses*

2013-24 ANÍBAL CORONEL, PATRICIO CUMSILLE, MAURICIO SEPÚLVEDA: *Convergence of a level-set algorithm in scalar conservation laws*

2013-25 SALIM MEDDAHI, DAVID MORA, RODOLFO RODRÍGUEZ: *Finite element analysis for a pressure-stress formulation of a fluid-structure interaction spectral problem*

2013-26 FABIÁN FLORES-BAZÁN, FERNANDO FLORES-BAZÁN, SIGIFREDO LAENGLE: *Characterizing efficiency on infinite-dimensional commodity spaces with ordering cones having possibly empty interior*

2014-01 ALFREDO BERMÚDEZ, DOLORES GÓMEZ, RODOLFO RODRÍGUEZ, PABLO VENEGAS: *Mathematical analysis and numerical solution of axisymmetric eddy-current problems with Preisach hysteresis model*